Cavitation inception speed study

ECHO Program study summary

The cavitation inception speed study was undertaken for the Vancouver Fraser Port Authority-led Enhancing Cetacean Habitat and Observation (ECHO) Program from February to December 2022. Using the ECHO Program's vessel source level database, this project evaluated whether the speed at which a vessel begins to produce cavitation could be estimated using five acoustic descriptors for commercial vessels transiting through the Salish Sea. This document summarizes the study's methods, key findings, and conclusions.

What questions was the study trying to answer?

Ship propeller cavitation occurs by the formation of gas-filled bubbles as the propeller quickly rotates through the water, causing low-pressure areas. When these gas-filled bubbles collapse, they emit noise. It is estimated that most of ships' underwater radiated noise is caused by cavitation. The cavitation inception speed study aimed to determine if it was possible to both identify cavitation in a vessel's acoustic signature, and from this, identify the speed at which cavitation is being produced. This study was conducted using both repeated underwater noise measurements of a single vessel, and by collecting and examining all underwater noise measurements of a specific vessel category.

The major questions that the ECHO Program hoped to address with this study included:

- Could cavitation inception be evaluated from readily available data and the acoustic noise spectrum of a vessel?
- Is the presence or absence of cavitation easily tied to an operating parameter such as speed through water?
- Is cavitation inception speed similar within a vessel category?

By identifying cavitation inception speeds, it may be possible to suggest a speed target that could provide the greatest underwater noise reduction benefit.

Who conducted the project?

The cavitation inception speed study was conducted by JASCO Applied Sciences Ltd. together with their subsidiary company DW Shipconsult, at the direction of the ECHO Program with funding support from Transport Canada.

What methods were used?

Based on a literature review of the changes to a vessel's acoustic spectrum due to cavitation, several potential descriptors were identified as possible indicators of cavitation. These were evaluated on a small subset of Bulker and Containership vessels which had a large number of measurements across a range of vessel speeds. This preliminary evaluation was intended to identify which potential acoustic descriptors would be appropriate to apply to a larger dataset of vessel measurements. For the main study, vessel data was only used under the following conditions:

- ECHO category: bulker, containership, tanker or vehicle carrier
- Nine or more measurements per vessel
- Vessel speed criteria was applied only for descriptors 1 and 4:
    - Descriptor 1 required a minimum speed through water ≤ 11.5 knots
    - Descriptor 4 required a minimum speed through water ≤ 10 knots and a maximum speed through water of ≥ 12 knots

Following preliminary analysis, the acoustic descriptors utilized included:

1. Descriptor 1 – Increase in low frequency cavitation hump seen from 20 - 80 Hz
   It is expected that the low frequency hump noise levels will increase with increased cavitation.
2. Descriptor 2 – Decrease in machinery tonal counts below 100 Hz
   As cavitation develops, machinery tonal signals which can be identified below 100 Hz in non-cavitating conditions, are expected to be masked by the cavitation. Thus, it is expected that tonal counts will decrease with increased cavitation.
3. Descriptor 3 – Decrease in slope of spectrum drop off from 2 kHz to 20 kHz
   It is expected that the negative slope of the vessel noise spectrum from 2 kHz to 20 kHz will become less negative as cavitation develops more fully.
4. Descriptor 4 – Factor X of URN increase relative to URN level at minimum measured speed per vessel
   A mathematical function was used to compare radiated noise levels in the 20-80 Hz range against the slowest speed radiated noise levels in the same frequency range. This mathematical function is described in the report in detail but generically called “Factor X”. It is expected that a vessels “Factor X” will increase with increased speed through water. (Similar to Descriptor 1 this change is symbolized by the red arrow in Figure 1 but evaluated differently from Descriptor 1)
5. Descriptor 5 – Confidence estimates of dual-band rotations per minute (RPM) estimator.
   JASCO has developed an acoustic estimator for propeller RPM. The estimator looks for harmonics of the shaft rate. Higher frequency harmonics are expected to be clearer with increased cavitation resulting in a higher confidence in finding harmonics at the upper frequency band. Conversely it is expected that increased cavitation will raise the background noise at lower frequencies resulting in a lower confidence interval when searching for harmonics in the low frequency band.
6. Descriptor 6 – Audio review and visual examination of spectrogram by experienced listener

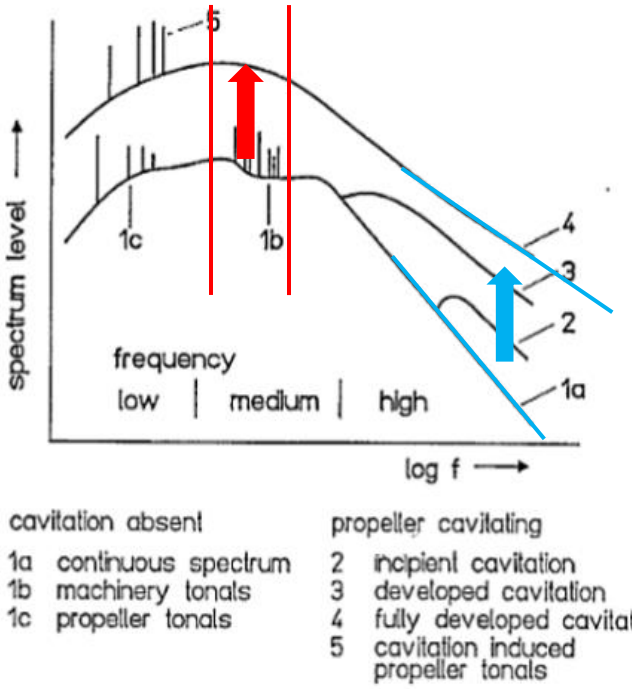

Descriptor 1 - Symbolized by frequency range bounded by the red lines and the move from spectral profile 1-3 to fully developed cavitation in spectral profile 4

Descriptor 2 - Machinery tonals are represented as spectral profile 1b and become less pronounced as cavitation becomes fully developed – spectral profile 4.

Descriptor 3 – Symbolized by the blue lines in Figure 1 moving from spectral profile 1a to 4

Descriptor 4 – This descriptor using a different mathematical evaluation of the same frequency range as descriptor 1 shown by the red lines and the movement from profile 1-3 to fully developed cavitation in spectral profile 4

***Figure** 1: Expected change in frequency spectrum as cavitation develops.*

Each descriptor was evaluated separately against the outcome expectation as noted above. From this, the descriptors were evaluated qualitatively. Descriptors that provided a definite estimate for cavitation inception speed, such as descriptor 1, were used to split vessel transits into two groups: those with speeds below the estimated cavitation inception speed and those above the estimated cavitation inception speed. These two groups were then compared using the results of the other “successful” descriptors. The expectation was that these two groups would show statistically significant differences when compared and that these differences would match the assumptions for cavitating and non-cavitating vessels as described above.

Lastly, acoustic reviews by an experienced operator were performed on 30 measurements from 10 vessels to help add insight to the efficacy of the descriptors.

What were the key findings?

The main findings of the cavitation inception speed study are summarized as follows:

- Descriptor 1, low frequency cavitation hump, yielded reasonable CIS estimates for individual vessels, but required multiple vessel readings over a range of speeds through water.
- Descriptor 2, machinery tonal counts, was able to note a trend in the aggregated data however there was significant overlap and this trending could only be seen when all vessel measurements were combined and binned by speed through water and the mean count evaluated.
- Descriptor 3, high frequency slope, focused on the expected change in slope of the vessel spectrum between 2 kHz and 20 kHz as cavitation develops, however, this relationship was not clear for all vessels. The relationship did reveal itself for vehicle carriers and containerships, however ulkers did not reveal this trend, and tankers demonstrated the opposite trend with increased speed.
- Descriptor 4, vessel “Factor X” showed a large amount of variability, and when vessels were grouped by vessel category there was no clear trend. This descriptor was considered not valid for the population of vessels considered.
- Descriptor 5, focused on the confidence interval of the dual-band RPM estimator. This descriptor did not show any relationship with speed and was not considered a good predictor of cavitation.
- Manual verification of 30 transits of 10 different vessels showed signs of cavitation in all but two transits - both of which occurred below 10 kts. It should be noted that cavitation was also seen in vessel speeds below 10 kts. The manual verification seems to indicate that true cavitation inception speed occurs at lower transit speeds that are typically observed in the ECHO Program dataset.
- Container Ships and vehicle carriers showed the most convincing results in detecting cavitation using the descriptors noted above. Bulkers showed mixed results and tankers had the least reliable results when compared to the expectations of the descriptors noted above.

Conclusions

The study showed that the descriptors chosen show some ability to detect cavitation, but only when reviewed with multiple measurements for the same vessel spanning a wide range of speeds through water. These descriptors, however, showed a wide range of cavitation inception speeds within a vessel category. As well, any individual vessel spectrum often showed variable results even when the same operational conditions were met. As a result, the results were considered more meaningful when considered as a distribution of possible cavitation inception speeds within a vessel category.

Of the descriptors evaluated, only Descriptor 1 and Descriptor 2 could provide an estimate of the speed where cavitation was estimated to occur. The estimated cavitation speeds for each vessel category, measured in knots as speed through water, are provided in the table below.

Descriptor	Tanker	Bulker	Container Ship	Car Carrier
#1	10.1 ± 1.1	11.2 ± 0.8	12.0 ± 2.3	11.0 ± 3.03
#2	N/A	N/A	12-13	12-13

It should be noted that both techniques may overestimate the speed at which true cavitation inception occurs as they require some level of developed cavitation to allow for the analysis technique to function. However, it is also likely that fully developed cavitation, in which noise source from cavitation dominates the spectrum, is likely to occur at a higher speed than indicated.

This study highlighted that there is a high degree of variability and uncertainty in the chosen descriptors that could only be distilled when considered in aggregate; either within a single vessel’s measurements or within all measurements within a vessel class. While the results provide valuable insight into the potential range of cavitation inception speeds for a vessel category, it is not considered a viable technique for the evaluation of a single vessel pass. As such, the ECHO Program does not intend to pursue the evaluation of cavitation inception speed further.

ECHO Cavitation Inception Speed Implementation Study

Phase 2 Technical Memorandum

JASCO Applied Sciences (Canada) Ltd

9 December 2022

Submitted to:

Derek White
Vancouver Fraser Port Authority
Contract 22-0238

Authors:

Jorge E. Quijano
Max Schuster
Alexander O. MacGillivray
Joshua N. Dolman
Johanna Daniel

P001703-001
Document 02929
Version 2.0

JASCO APPLIED SCIENCES

Suggested citation:

Quijano, J.E., A.O. MacGillivray, J.N. Dolman, M. Schuster, and J. Daniel. 2022. ECHO Cavitation Inception Speed Implementation Study: Phase 2 Technical Memorandum. Document 02929, Version 2.0. Technical report by JASCO Applied Sciences for Vancouver Fraser Port Authority.

Author Affiliations:

JASCO Applied Sciences
Jorge E. Quijano
Alexander O. MacGillivray
Joshua N. Dolman

DW-ShipConsult GmbH
Max Schuster
Johanna Daniel

Contents

Figures

Tables

1. Introduction

This technical memorandum describes an investigation into the cavitation inception speed (CIS) of commercial shipping vessels using underwater radiated noise (URN) measurements from the Enhancing Cetacean Habitat and Observation (ECHO) program source level database. The objective of this study is to investigate acoustic descriptors developed for estimating cavitation inception speed for commercial vessels transiting through the Salish Sea and calling at the Port of Vancouver. These acoustic descriptors were derived from technical vessel characteristics, transit speed, and radiated noise spectrum features, with the intent of using the descriptors to improve present speed limits and recommendations for the ECHO slowdown mitigation measures. By applying these descriptors to the large ECHO source level database, CIS estimates may be developed for different vessels to help inform voluntary slowdown speeds to better reduce the impact of URN on local marine mammals.

Cavitation from vessel propellers contributes significantly to overall background noise in the sea. Slowing transiting vessels to operate below CIS would reduce radiated vessel noise in critical habitat areas of importance to Southern Resident killer whales. This study was undertaken in two phases. The first phase demonstrated the feasibility of cavitation descriptors for a limited subset of vessels (Daniel et al. 2022), and the second applied statistical analysis of the most promising descriptors to a larger URN data set. This report focuses on the second (implementation) phase of the study, using URN measurements from a broader selection of commercial vessels from the ECHO source level database to evaluate the most promising acoustic descriptors identified during the first (feasibility) phase.

During the feasibility study, a literature search was carried out to understand the mechanisms responsible for generating underwater cavitation noise. During that initial investigation, two types of descriptors were defined: operational and noise descriptors. The descriptors were tested using a set of URN measurements for the 100 most-frequently measured vessels in the ECHO data set. Vessels analyzed in Phase 1 were limited to those Bulkers and Container Ships that were measured on more than 19 occasions.

1.1. Operational Descriptors

Operational descriptors are variables that summarize one or several characteristics of a vessel and its operation parameters. The expectation of an operational descriptor suitable to investigate CIS is that, when used as the independent variable to describe the increase of noise in cavitation-impacted bands, it would reveal a clear transition from a non-cavitation into a cavitation regime.

In Phase 1, the following operational descriptors were considered: draft ratio, advance ratio, propeller loading, propeller tip speed, cavitation number, block coefficient, Froude number, Reynolds number, shaft rate, and speed through water (STW). From these operational descriptors, STW was found to be the most relevant because it is a reliable quantity available in the ECHO database for most vessels (see Section 2.1 for a description of the STW calculation by ShipSound).

Regarding the other operational descriptors, the following conclusions were reached:

- Draft ratio, advance ratio, propeller loading, propeller tip speed, cavitation number, and block coefficient had the shortcoming of requiring vessel characteristics generally unavailable in the ECHO database (i.e., propeller diameter, design draft, vessel hull dimensions), and therefore certain assumptions were required for estimating them.
- Because the Froude and Reynolds numbers are proportional to STW, no advantage was found in using them as operational descriptors.
- Shaft rate was estimated in the ECHO database using JASCO's dual band DEMON estimator (JASCO Applied Sciences and SMRU Consulting 2020). Although the estimator was shown to perform well, there are still cases in which the acoustic signal presents challenges, resulting in unreasonably high shaft rate estimates (sometimes corresponding to a propeller rate, rather than a shaft rate). For this reason and also because it is known that shaft rate is strongly correlated to STW, for each vessel, this operational descriptor was not pursued further.

1.2. Noise Descriptors

Noise descriptors are variables intended to identify cavitation-generated features in both narrow-band spectrum and wide-band source levels (SLs). In Phase 1, the following noise descriptors were analyzed:

- Increase in low-frequency broadband noise as a function of STW. The descriptor was explored using the monopole source level (MSL) for several bands (see Section 2.3.1).
- Masking of tonal engine noise by cavitation noise (see Section 2.3.2).
- Slope of the spectrum in the 0.1–20 kHz and 2–20 kHz frequency bands as a function of STW (see Section 2.3.3).
- Slope X of the SL as a function of $\log_{10}(STW)$. The descriptor was explored for an SL obtained within various bands (see Section 2.3.4).

In addition, URN measurements were manually analyzed to identify cavitation from the raw audio signal. This approach, however, is unsuitable for larger data sets because it must be performed in a case-by-case basis by a trained analyst. The results in Phase 1 of this study identified the most promising noise descriptors, which were further refined in using a more comprehensive set of URN measurements from the ECHO database, as described in Sections 2–4.

2. Methods

2.1. Data Set Description

The ECHO vessel noise database, which contains many thousands of vessel measurements, was the primary source of statistical URN data used in this study. These data have been collected since 2015 on underwater listening stations (ULSs) in Boundary Pass, Haro Strait, and Strait of Georgia (see Figure 1). URN measurements from the ECHO database were collected using the ShipSound component of JASCO's PortListen® system (see Appendix A). The ECHO database combines URN measurement data from hydrophones with AIS data transmitted by vessels. The acoustic data are stored as decidecade band source levels and narrowband spectral density levels. ShipSound also stores raw audio files for acoustic analysts to inspect. These acoustic data are matched to AIS information about the operational state of a vessel at the time of measurement, such as STW, draft, heading, and vessel specifications from AIS such as overall length, breadth, and deadweight tonnage. JASCO's dual-band DEMON algorithm was applied to the acoustic data to determine the propeller shaft rate.

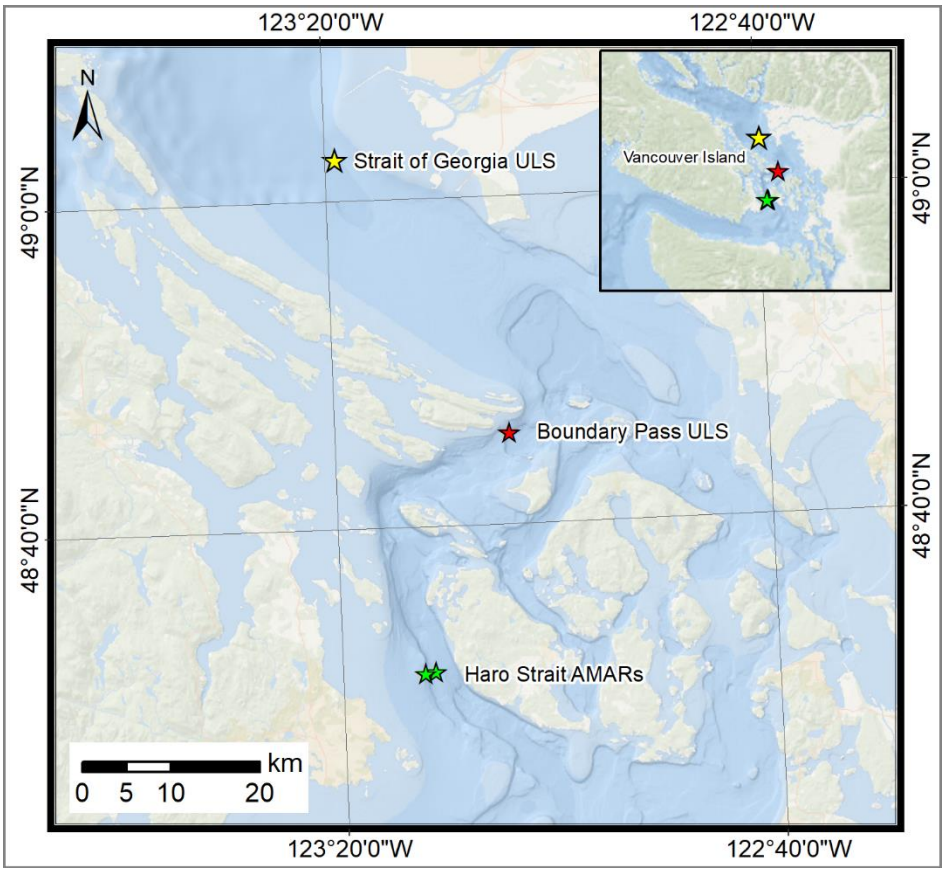

Figure 1. Map showing locations of underwater listening stations (ULSs) where Enhancing Cetacean Habitat and Observation (ECHO) source level (SL) measurements were collected from 2015–2022.

The STW was computed by ShipSound as the vector difference between the speed over ground (from AIS) and the ocean current (Figure 2). Where possible, ocean current data were measured near the sea surface using an Acoustic Current Doppler Profiler (ADCP) deployed at the Strait of Georgia and Boundary Pass stations. For measurements where direct ocean current measurements were unavailable (e.g., in Haro Strait and during 2019 in Boundary Pass), ocean current data were estimated using the WebTide Tidal Prediction Model (v 0.7.1) provided by Fisheries and Oceans Canada (Bedford Institute of Oceanography 2015).

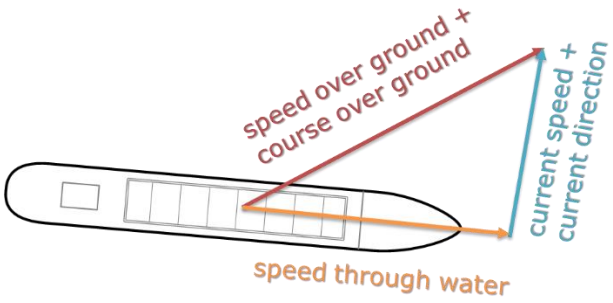

STW vector = SOG vector - current vector

Figure 2. Diagram of speed through water calculation (STW = speed through water, SOG = speed over ground).

During the Phase 1 feasibility study, the performance of the CIS descriptors was evaluated using a limited subset of URN measurements, consisting of data for the most-frequently measured Bulker Carriers and Container Ships in the ECHO data set. For the current study (Phase 2), the analysis was expanded to include four vessel categories:

1. Bulk carriers,
2. Container Ships,
3. Tankers, and
4. Vehicle Carriers.

The ECHO database contained 24,741 QC-accepted measurements for vessels in these four categories, collected over the approximately 7-year period between September 2015 and July 2022. The following steps were carried out to ensure the quality of the data used in this analysis:

1. Visual inspection of scatter plots of design characteristics and a search algorithm were used to identify cases of vessels in the database with multiple MMSI numbers, with missing IMO numbers, or with mislabeled vessel categories. In all cases, the identified errors were manually corrected by cross checking vessel characteristics against online databases.
2. MSL was used to quantify URN. MSL is a **source level** that has been calculated using an acoustic model that accounts for the effect of the sea surface and seabed on sound propagation, assuming a **point source** (monopole). The calculated source level depends on the source depth, which is taken to be 70 % of the vessel draft at the time of measurement, per ISO standard 17208-2 (2019). Measurements in the ECHO data set collected prior to publication of the 2019 standard were calculated assuming a source depth equal to 50 % draft. To address this inconsistency, decidecade-band source levels for pre-2019 measurements were adjusted to a standard 70 % draft value using formulae provided in Annex A of ISO 17208-2, following the procedure described in MacGillivray and de Jong (2021).

2.2. Vessel Selection

During the Phase 1 feasibility study, measurements to develop and test cavitation descriptors were selected by applying bounds to the minimum vessel speed ($V_{Min} \leq$ 14 kn), the difference between maximum and minimum speed ($V_{STW,Max} - V_{STW,Min}$ > 5 kn), the difference between the maximum and the minimum broadband MSL ($L_{S,max} - L_{S,min}$ greater than 15 and 10 dB for Container Ship and Bulker categories, respectively), the Pearson correlation coefficient between L_S and V_{STW} ($r > 0.5$), and a minimum of 19 measurements per vessel category. Such criteria were intended to provide sufficient measurements for robust statistical analysis of the cavitation descriptors, while at the same time highlighting features on which the descriptors would focus.

For the current study (Phase 2), the selection criteria applied to vessels in the ECHO database was relaxed since the goal was to test the validity and robustness of the Phase 1 descriptors on a larger and more generalized data set, this time also including Tankers and Vehicle Carriers. For this work, vessels with nine or more measurements were included. This threshold was chosen as a compromise between maximizing the total number of unique vessels and having enough measurements per vessel for robust statistical analysis. For descriptors 1 and 4, the data were limited to measurements with $V_{STW,Min} \leq$11.5 kn and $V_{STW,Min} \leq$10 kn, respectively, since those descriptors rely on data at low speeds to indicate trends from low to high cavitation. In addition, for descriptor 4 only measurements with $V_{STW,Max} \geq$12 kn were used. Although the Pearson correlation coefficient between L_S and V_{STW} was not included as a selection criteria, most of the selected Container Ship and Vehicle Carriers had $r > 0.5$, most Bulkers had $r > 0.25$, and most Tankers had $r > 0.125$ (Figure 3).

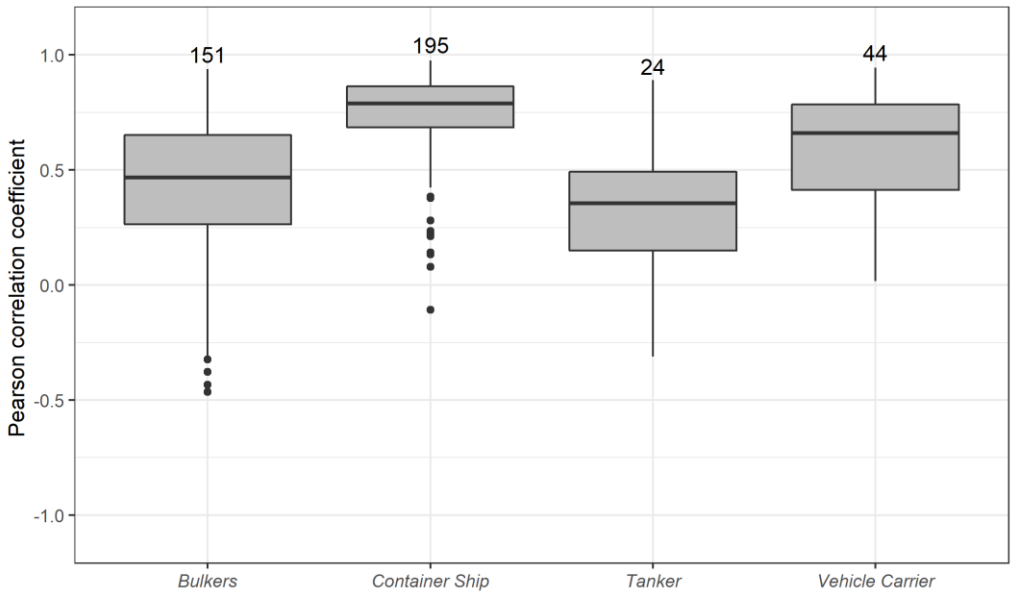

Figure 3. Pearson correlation coefficient between broadband MSL (L_S) and V_{STW} for the selected vessels in the current study (Phase 2).

The Boundary Pass station data were collected at two closely spaced ULS frames, so it is common to find replicate measurements of the same vessel (i.e., the same vessel transit measured almost simultaneously at the two ULS) after 2019. The selection criteria of nine or more measurements only considered unique Boundary Pass measurements. However, once a vessel was selected, replicate Boundary Pass measurements were included in the final data set.

2.3. Cavitation Descriptors

As discussed in the Phase 1 report, cavitation significantly affects the radiated noise spectrum of a marine vessel. At the cavitation inception speed, the spectrum starts to increase at the higher frequencies. Because cavitation effects become stronger at higher vessel speeds, the peak of the cavitation tends to shift to lower frequencies, up to the point at which it starts competing (and even masking) the discrete machinery tonals commonly seen at frequencies <100 Hz. Figure 4 shows the following contributions of cavitation on the source level spectrum of a typical passing vessel at different speeds:

- **Condition 1**: Cavitation is absent in at low speed. Spectrum components 1a, 1b, and 1c are attributed to non-cavitating propeller, machinery tonals, broadband noise from bow waves breaking, and other hydrodynamic sources.
- **Condition 2**: Broadband cavitation begins at high frequency as vessel speed increases. The speed at which cavitation begins is called the cavitation inception speed (CIS) and is an important value for this study.
- **Condition 3**: As vessel speed and propeller loading increase from condition 2, the extent of cavitation increases. As a consequence, the level increases and peak frequency shift to a lower frequency.
- **Condition 4**: Until cavitation has fully developed, the range at which cavitation is dominant further decreases to lower frequencies. This peak frequency will not change further once all dominant types of cavitation appear in a stable condition. Higher ship speed above this condition only affects the radiated level, with negligible impact on the spectral shape.
- **Condition 5**: Eventually, the machinery noise found at medium frequencies (1b) is masked by cavitation noise. Low-frequency blade rate tonals are present throughout this process, with tone intensity increasing strongly as an effect of cavitation.

This section explains how each of the proposed cavitation descriptors attempts to exploit specific spectral features to detect the presence of cavitation.

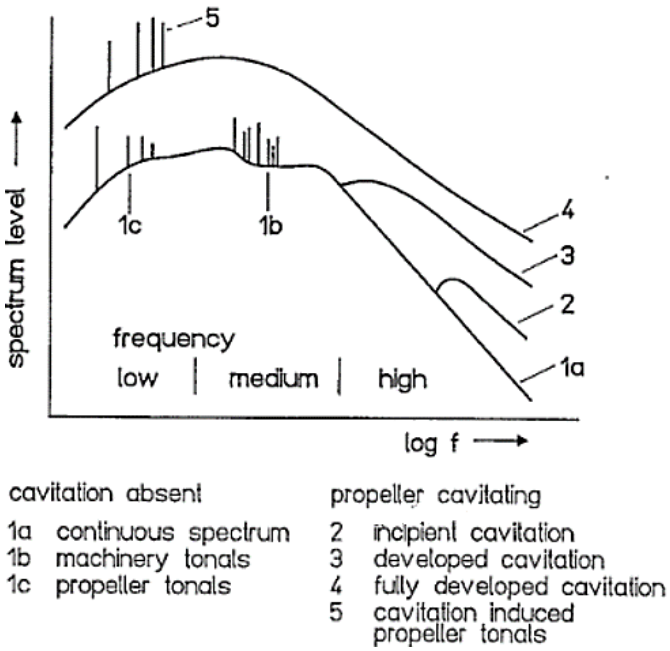

Figure 4. Cavitation noise impact on a typical noise spectrum for a transiting vessel (source: Baiter 1992).

The types of cavitation that occur on a propeller are strongly influenced by individual design features of the propeller blades such as pitch distribution and skew. Therefore, as propellers are individually designed for each ship, a general statement on what types of cavitation develop in which order cannot be made. However, the formation process over ship speed of all cavitation types as shown in Figure 5 can be generalized:

1. Incipient cavitation of each cavitation type is characterized by the sporadic occurrence of bubbles. As the inflow of the propeller and spatial distribution of cavitation nuclei can be inhomogeneous in the inflow of a propeller, the occurrence of the first bubbles is very random and unstable. These bubbles are very small and exist only for a short time period. Acoustic emissions by means of modulated high-frequency broadband sound of incipient cavitation are primarily caused by the collapse of these microscopic bubbles.
2. Developed cavitation is characterized by the stable existence of larger bubbles that appear over a larger rotation angle of the propeller. Figure 6 and Table 1 illustrate the growth and collapse of a stable sheet cavity. Correspondingly, this formation over blade rotation is applicable to other types of cavitation. Sheet cavitation and tip vortex cavitation are the most frequently observed types on merchant ship propellers. The stable existence of large cavities is required to radiate low-frequency sound.

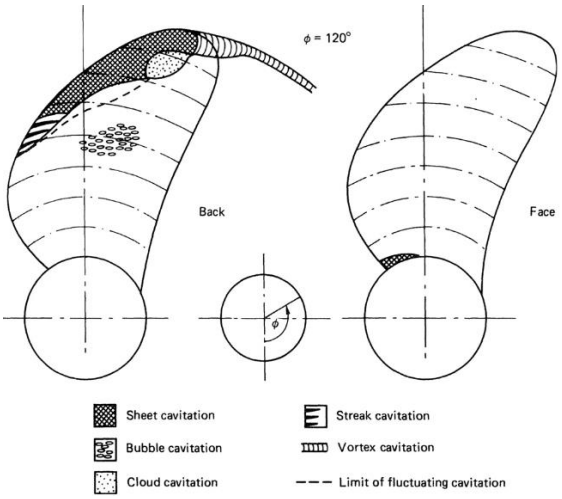

Figure 5. Illustration of types of cavitation Source: Carlton (2012).

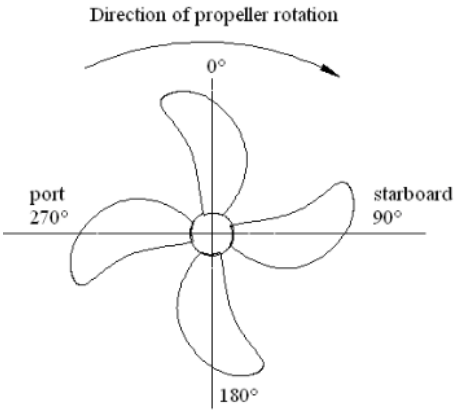

Figure 6. Coordinate systems for illustration of cavitation pattern in Table 1 according to Zheng et al (2019).

Table 1. Illustration of fully developed, stable, sheet cavitation, adapted from Zheng et al (2019), with coordinates according to Figure 6.

-10°	0°	10°	20°	30°	40°	50°
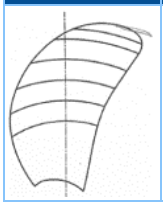	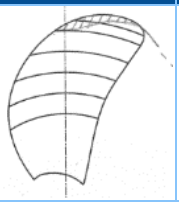	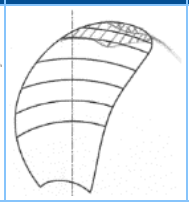	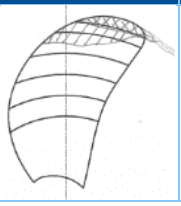	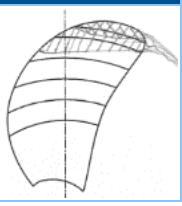	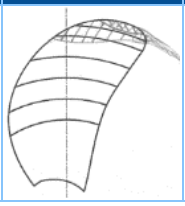	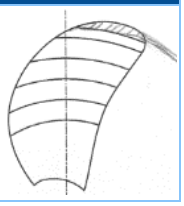

2.3.1. Descriptor 1: Increase in Low-Frequency Cavitation Hump (20-80 Hz)

When cavitation is well developed, the cavitation hump shifts to the lowest frequencies, resulting in an increase in the broadband noise levels below 100 Hz. In the absence of cavitation, the low-frequency spectrum is usually dominated by machinery noise (e.g., propeller and shaft harmonics). For this descriptor:

- We hypothesize that CIS can be identified when the cavitation noise exceeds the machinery noise by a certain threshold.
- Because the peak of the cavitation hump amplitude typically occurs between 30–50 Hz, we explored the relation between vessel speed and MSL for multiple bands (31, 50, and broadband 20–80 Hz). We concluded that a broadband level within ~20–80 Hz represents the impact of cavitation better than individual decidecade bands.

Given our hypothesis, our analysis also proposes a simplified noise model to be fit to the data, from which the transition between machinery-dominated noise below CIS and cavitation-dominated noise above CIS can be deduced. The model consists of a constant machinery noise level L_M and a speed-dependent cavitation level L_C:

$$L_M = C_1 \text{ and} \tag{1}$$

$$L_C(v) = C_2 + n \times 10\log_{10}\left(\frac{v}{v_{ref}}\right), \tag{2}$$

where C_1 represents an idealized constant machinery noise level, C_2 is the cavitation noise level at the reference speed v_{ref} (arbitrarily taken to be 10 kn), and n is a power-law exponent that indicates how the cavitation noise increases with the vessel speed v. In this equation, vessel speed is measured in terms of the STW, as discussed in Section 1.1. The total source level (L_S) is given by the power summation of these two terms:

$$L_S(v) = 10\log_{10}\left(10^{L_M/10} + 10^{L_C(v)/10}\right). \tag{3}$$

Table 2 summarizes the parameters for the proposed vessel noise model.

Table 2. Summary of the parameters used in the non-linear monopole source level (MSL) model in Equation 3.

Parameter	Unit	Interpretation
C_1	dB	Vessel noise level due to mechanisms unrelated to cavitation, usually dominated by machinery noise. To simplify the model, it is idealized here to be a constant independent of vessel speed.
C_2	dB	Cavitation noise level at the reference speed v_{ref}.
n	dB/decade	Rate of increase of cavitation noise level with speed. For example, at 10 times the reference speed (i.e., one decade), the cavitation noise level is $C_2 + 10n$.

Figure 7 illustrates the interaction between the machinery and the cavitation noise components in this model. At low vessel speed (below CIS), the machinery component dominates. Above CIS, the cavitation component becomes louder than the machinery, resulting in a rapid increase in noise emissions with speed.

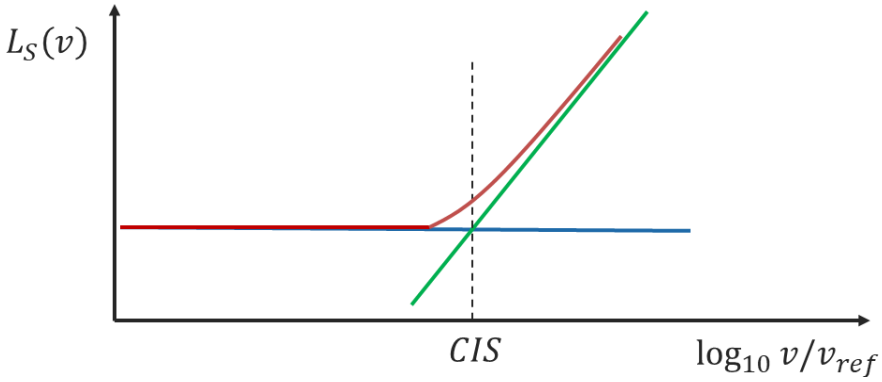

Figure 7. Illustration of the simplified machinery (blue) and cavitation (green) noise model used in this work. Total noise (red) is the summation of the machinery and cavitation components. Cavitation Inception Speed (CIS) is estimated to occur at the speed where machinery noise and cavitation noise lines intersect (i.e., where $L_c(v) = L_M$).

Equation 3 is a non-linear model, which means that it cannot be fit to data using standard linear regression techniques. To overcome this issue, we applied a non-linear least squares (NLS) algorithm to find a fit of this model to the low-frequency broadband MSL for each vessel category, using the NLS package in version 4.0.2 of the R language (R Core Team 2020).

The NLS algorithm operates by searching a three-dimensional (3-D; i.e., $C_1, C_2,$ and n) parameter space for an optimal fit to the data. In this search process, the input parameters are varied simultaneously. For each variation, the NLS algorithm computes the difference between the model in Equation 3 and the data as the mean square error, defined as:

$$MSE(C_1, C_2, n) = \frac{1}{N}\sum_{n=1}^{N}\left(L_S(v_n) - L'_{S,n}\right)^2 \quad (4)$$

where N is the total number of MSL measurements (i.e., the number of data points), $L'_{S,n}$ is the n^{th} MSL measurement, and v_n its corresponding STW. The goal of the NLS algorithm is to find a particular combination of C_1, C_2, and n that minimizes the MSE defined in Equation 4.

The advantage of this approach is that it yields best fit estimates of the model parameters C_1, C_2, and n, such that we can define CIS as the speed when the cavitation noise level is equal to the machinery noise level. The disadvantage of the NLS approach is that it is not guaranteed to converge to an optimal fit, and therefore it is not always possible to obtain an estimate of the model parameters for a given data set.

Since this approach requires data at both low and high speeds to properly constrain the fit, this descriptor was only applied to vessels with $STW_{min} \leq 11.5$ kn. By applying this condition, the data set used to evaluate this descriptor was reduced to a total of 191 unique vessels (117 Bulkers, 47 Container Ships, 12 Tankers, and 15 Vehicle Carriers).

2.3.2. Descriptor 2: Number of Tonals Below 100 Hz

In addition to the MSL hump exploited by Descriptor 1 (see Section 2.3.1), the cavitation noise also tends to mask the narrow-band machinery harmonics commonly observed at frequencies <100 Hz. This is shown in Figure 8, which compares the number of narrowband harmonics between ~40–100 Hz at low and high STW for the same Container Ship. For this descriptor:

- We hypothesize that the number of discrete tonals in the band of interest can be used to indicate the presence or absence of fully developed sheet or vortex cavitation (Figure 5). A large number of tonals (Figure 8 left) indicates low cavitation, while a reduction in the number of tonals (Figure 8 right) indicates high cavitation masking the tonals.
- The tonal count approach was explored for multiple frequency bands, with the 10–100 Hz band yielding the best results.
- The tonal count was performed using the same automatic tone-detection algorithm as in Phase 1 (i.e., by identifying tones as narrowband spectrum values that exceed the median-smoothed spectrum by a certain threshold). Three thresholds were explored for detecting tonal peaks, and the algorithm's performance for each threshold was evaluated by visual inspection of the spectra and tone detections (such as in the example in Figure 8) for multiple measurements. The following results were obtained:
  - 3 dB above the background level: This threshold resulted in a large number of detections, some of them likely not tonals but rather oscillations of the background noise.
  - 6 dB above the background level: This threshold provided the best results for this descriptor because it represents a trade-off between maximizing the number of detected tonals and minimizing the number of false (background noise) peaks.
  - 9 dB above the background level: This threshold resulted in a smaller number of detections, most of them corresponding to true tonals. However, with such a high threshold, true harmonics with small amplitudes can go undetected.

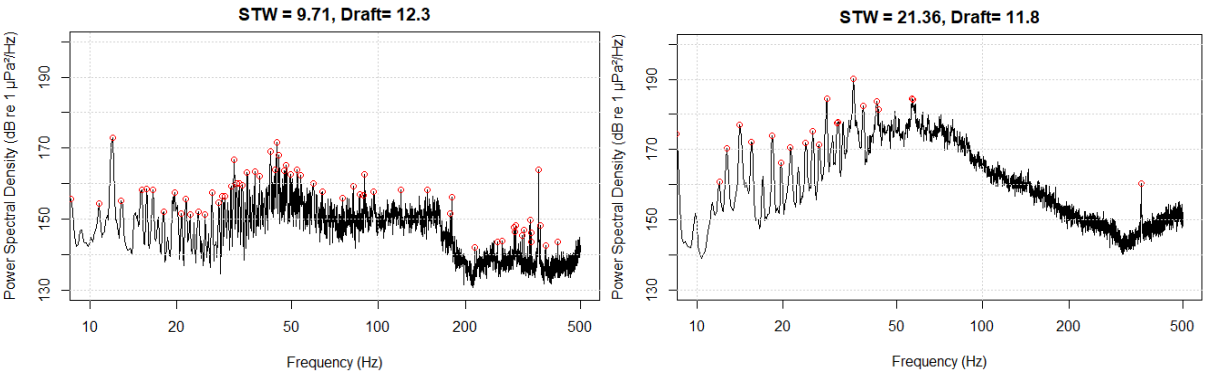

Figure 8. Example of masking on machinery tonals in a container ship: (Left) Example of a spectrum with no cavitation at low speed through water (STW; 9.7 kn) and (right) a spectrum with high cavitation, corresponding to STW (21.3 kn). Red circles indicate narrowband harmonics, which were detected by an automatic tone-detection algorithm with a 6 dB threshold. Only the detections below 100 Hz were considered for Descriptor 2.

2.3.3. Descriptor 3: Spectral Slope

The spectral slope descriptor investigates the decay rate of the spectra at higher frequencies. Because cavitation onset manifests itself as a hump at high frequencies and then gradually shifts to lower frequencies (see Figure 4), the decay rate of the spectra as a function of vessel speed can offer insight into when cavitation occurs. For this descriptor:

- We hypothesize that at low speeds (prior to or at very low cavitation), the spectrum has a steep decay compared to cases at high speed (when cavitation is well developed). Figure 9 shows an example of this effect for the same vessel at two speeds.
- We performed a linear fit to the 1 Hz spectrum, after removing the narrowband tonals by applying an 81-point median smoothing filter. We explored this fit over two frequency bands: 0.1–20 and 2–20 kHz. The results for the 0.1–20 kHz band yielded the most promising results.
- In all cases, the spectrum frequency was presented to the fit algorithm on a logarithmic scale. To avoid biasing the fit by the (more numerous) high-frequency data, the frequency scale was uniformly sampled in log space.

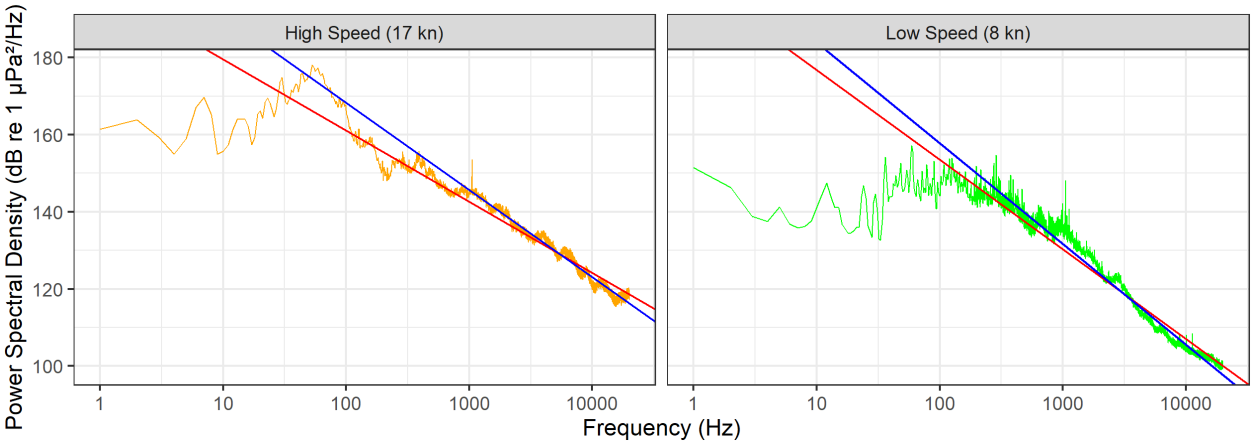

Figure 9. Example of vessel noise spectra at: (left) High speed through water (STW; 17 kn); and (right) low STW (8 kn). Linear fits to for 2–20 and 0.01–20 kHz are shown as solid blue and red lines, respectively. The slope of the linear fit is used by Descriptor 3 to determine the presence of cavitation.

2.3.4. Descriptor 4: Factor X of URN Increase Relative to Speed

Figure 10 illustrates the operation of Descriptor 4. When plotting the MSL as a function of log speed, the goal is to compute the local slope X from the minimum speed data point (shown in red in Figure 10), to each of the other points in the ensemble. From this idealized illustration, it is clear that X should remain closer to a small value for data at lower speeds (and presumably, before cavitation), while it should increase in value for data at high speeds. For this descriptor:

- We hypothesize that at low speeds (before cavitation takes place), X should remain at a low value compared data at high speeds once cavitation drives the MSL to much higher values.
- Numerically, X is computed using the equation for the slope of a straight line, as follows:

$$X = \frac{L_S(v) - L_S(v_{min})}{\log_{10} v - \log_{10} v_{min}}$$

  where $L_S(v)$ is the MSL in a given frequency range at speed v.
- Several low-frequency bands were explored for the definition of MSL. The results presented here correspond to the broadband MSL in the 20–80 Hz range, a frequency range known to be affected by cavitation.
- For investigating the Slope X descriptor, the URN data set was further filtered to include only vessels for which $v_{min} \leq 10$ kn and $v_{max} \geq 12$ kn, to allow a sufficient speed range to investigate the anticipated speed dependence.

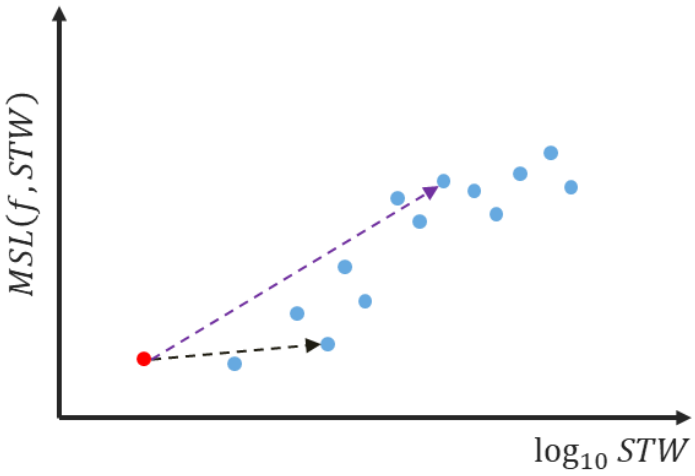

Figure 10. Estimation of the local slope from the point of minimum speed (red) to other data points: The slope for the purple dashed line toward data with high cavitation is steeper than the slope of the black dashed line toward data with lower speed and without cavitation.

2.3.5. Descriptor 5: Confidence of Dual-band RPM Estimator

JASCO'S dual band RPM estimator operates on two frequency bands: low-band (LB) estimator (0–40 Hz) and DEMON estimator (10–30 kHz). Each of these estimators analyze the separation between harmonic peaks, by testing how many of those peaks support a proposed shaft RPM. For example, for a shaft RPM of 2 Hz, we expect to find harmonic peaks at 2 Hz and at multiple frequencies of 4 Hz, 6 Hz, etc. During its development, JASCO's RPM estimator included computation of LB and DEMON confidence factors (CF_{LB} and CF_D, respectively) ranging from 0 % for low confidence to 100 % to high confidence. These confidence factors were tuned to quantify the confidence on the RPM estimator, and they depend on the following factors:

- The number of harmonics that agree with the hypothesis of the estimated RPM.
- The quality of the low-frequency or the DEMON spectra: low-quality spectra would have low amplitude peaks that are easily confused with background noise, while a high-quality spectra would have peaks well above the background noise.

For the purpose of detecting cavitation, our hypothesis is that:

- At very low speeds (before cavitation takes place), the DEMON confidence factor CF_D would be low since the DEMON spectrum (which depends on cavitation) would not exhibit the characteristic cavitation modulation peaks.
- At moderate and high speeds when cavitation develops, the CF_D would be higher as a result of a high-quality spectrum with clear harmonic peak structure. The low-band estimator would yield high confidence CF_{LB} at low speeds, when cavitation is weak and it mostly affects the high-frequency portion of the spectrum. However, at very high speeds estimation of the harmonic structure in the 0–40 Hz should be affected by cavitation, which would tend to increase the background noise in the spectra and make it difficult to detect harmonic peaks. Consequently, the confidence factor for the low-frequency estimator would be low.

2.4. Manual Validation

Manual validation is performed on URN measurements to identify typical features associated with cavitation noise. The results from this manual validation can be compared to those from the cavitation inception speed descriptors proposed in this work. The manual validation relies on the experience of a human sonar analyst to identify individual noise-generating mechanisms on a ship, by hearing and spectrogram analysis.

To support the overall objective of this project on cavitation inception, it is primarily required to assess whether cavitation is present. This information can be concluded by separating the noise contribution from on board machinery to that of in-water noise by cavitation. In this context, cavitation inception refers to the operating condition of a ship, where cavitation noise becomes detectable in the presence of various machinery noises. Therefore, in cases of noisy machinery, incipient cavitation is likely to be masked, until sufficiently developed cavitation noise dominates the machinery noise. One particular challenge for acoustic identification of incipient cavitation in presence of machinery noise is on determining the affected frequency range where incipient cavitation can be detected by modulated sounds caused by individual blades. Many two-stroke engines radiate very similar sounds at similar levels in the affected frequency range that can only be differentiated from incipient cavitation by auditory impression or by investigating modulation patterns (i.e., whether the modulated noise is consistent with the number of cylinders or propeller blades). So far, both procedures to differentiate two-stroke machinery sounds from sounds of incipient cavitation can only be performed by a human analyst. These manual procedures are successful in many situations, even when automated detectors that make use of changes in spectral slope cannot reliably identify incipient cavitation due to the very small increase of level.

Manual analysis makes use of human hearing perception capabilities in combination with visual analysis of spectrograms and narrow band spectra. Despite some capabilities of the hearing and spectrum analysis approaches being redundant, the two methods are powerful when applied in combination because each of them has the following unique strengths:

- Spectrogram analysis can be used to visualize tonal components that are not detected by the human ear due to presence of masking sounds within a critical band (Seeber 2008). In addition, the frequency range of spectrogram analysis is only limited by frequency content of the recorded signal (Nyquist criterion linked to sampling rate) while the human ear is limited to a frequency range of approximately 20 Hz to 20 kHz. For all recordings of ECHO data, spectrograms can yield additional information beyond 20 kHz that is affected by sounds of incipient cavitation (Hosien and Selim 2017).
- Audio analysis provides a quick assessment of the overall noise characteristic (e.g., presence of tonal or broadband components, presence of modulated sounds, impulsive events, repetitive components). Audio analysis is particularly powerful when interpreting periodic components, such as the characteristic noise of rotating propeller blades or ignition of cylinders in a two-stroke engine. Especially at the threshold of cavitation inception, some blades tend to cavitate earlier than others so that they appear louder. This creates a distinct rhythm that is perceived more easily by listening than by spectrogram analysis.

In this work, audio files for thirty URN measurements were investigated by an experienced human analyst to validate cavitation inception speed estimates.

2.5. Vessel Selection

After applying the vessel selection criteria described in Section 2.2 to the ECHO database, the data set for evaluating the CIS descriptors was reduced to 414 unique vessels, including 151 bulkers, 195 container ships, 24 tankers, and 44 vehicle carriers. In total, the data set included 8706 individual URN measurements. For each vessel category, Figures 11–14 provide histograms showing the number of unique vessels versus the number of unique and replicate measurements. Container ships and bulkers were by far the most frequently measured vessels in the data set, comprising 53 % and 30 % of the total measurements, respectively.

Vessels included in this data set represented a wide range of draft, length, and STW conditions (Figures 15–17, Table 3) and a minimum of nine unique measurements. Previous work demonstrated that STW, actual draft, and ship length are significantly correlated with vessel noise (MacGillivray et al. 2022). Unfortunately, many other vessel properties of interest to this study, such as propeller and engine specifications, are held proprietary by vessel operators and manufacturers so those properties were unavailable for this study.

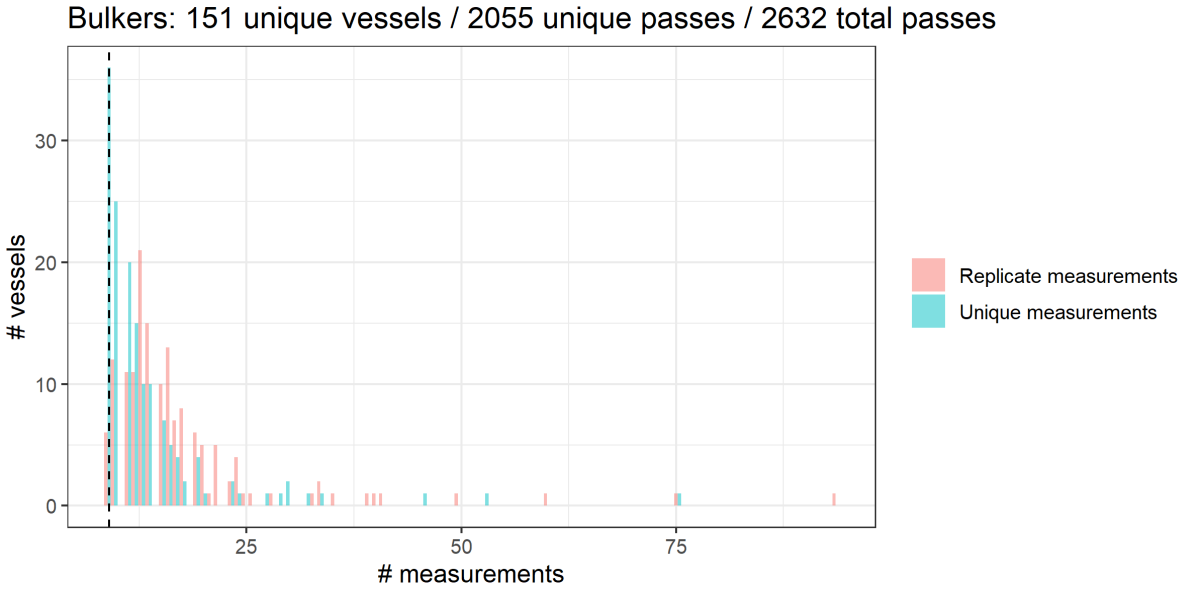

Figure 11. Histogram of the number of unique Bulkers versus the number of measurements in the data set selected for this study. The vertical dashed line indicates the minimum of 9 unique measurements used for selection of test cases.

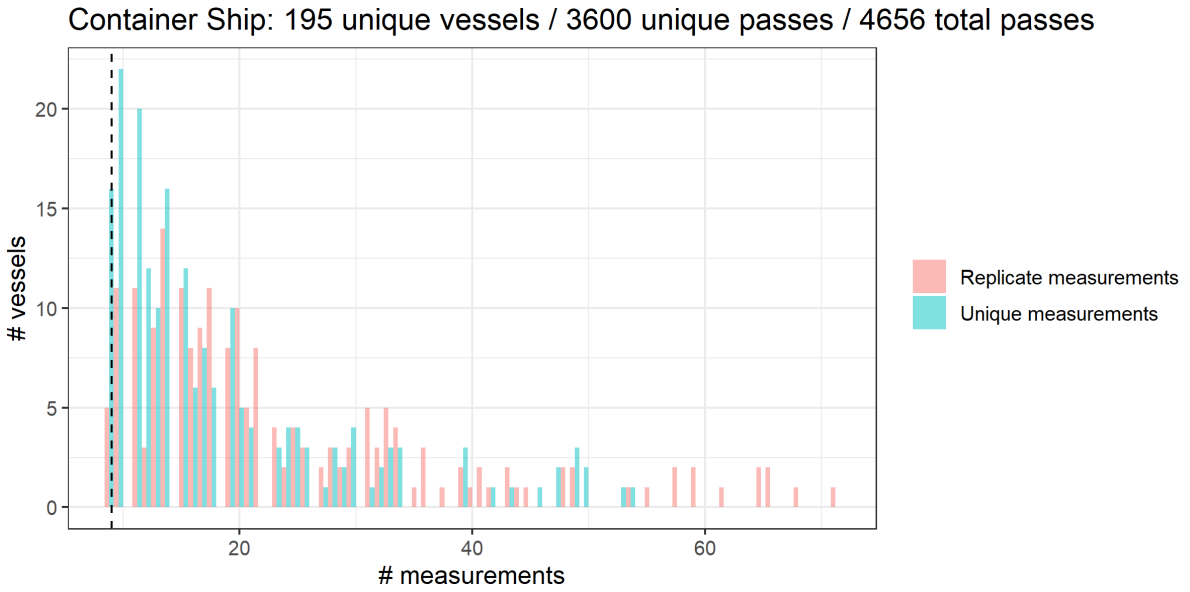

Figure 12. Histogram of the number of unique Container Ships versus the number of measurements in the data set selected for this study. The vertical dashed line indicates the minimum of 9 unique measurements used for selection of test cases.

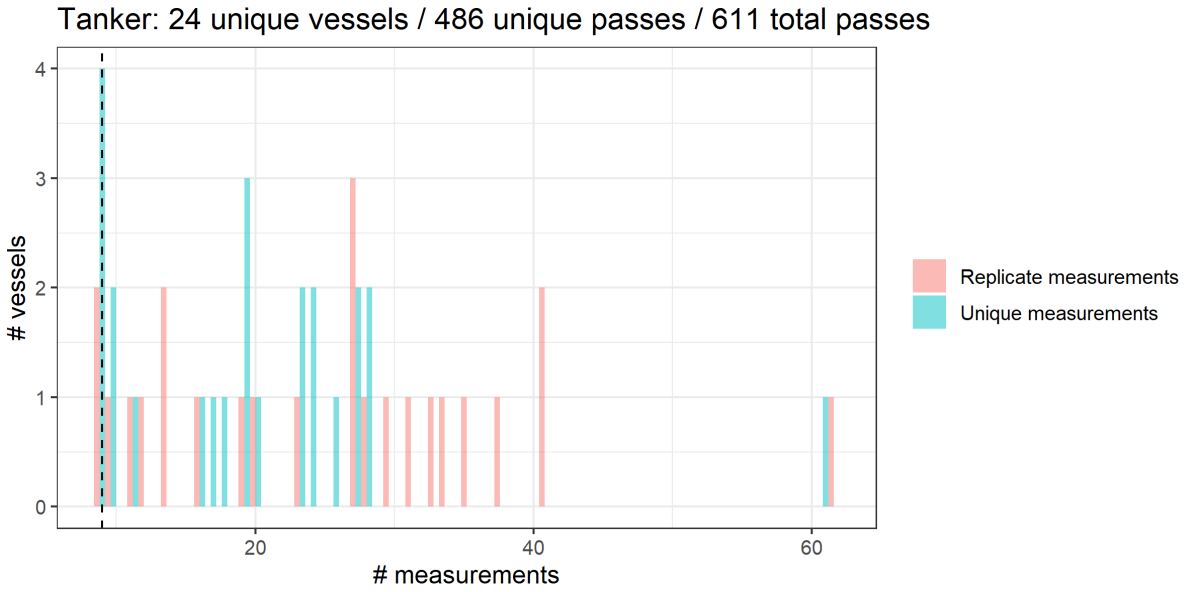

Figure 13. Histogram of the number of unique Tankers versus the number of measurements in the data set selected for this study. The vertical dashed line indicates the minimum of 9 unique measurements used for selection of test cases.

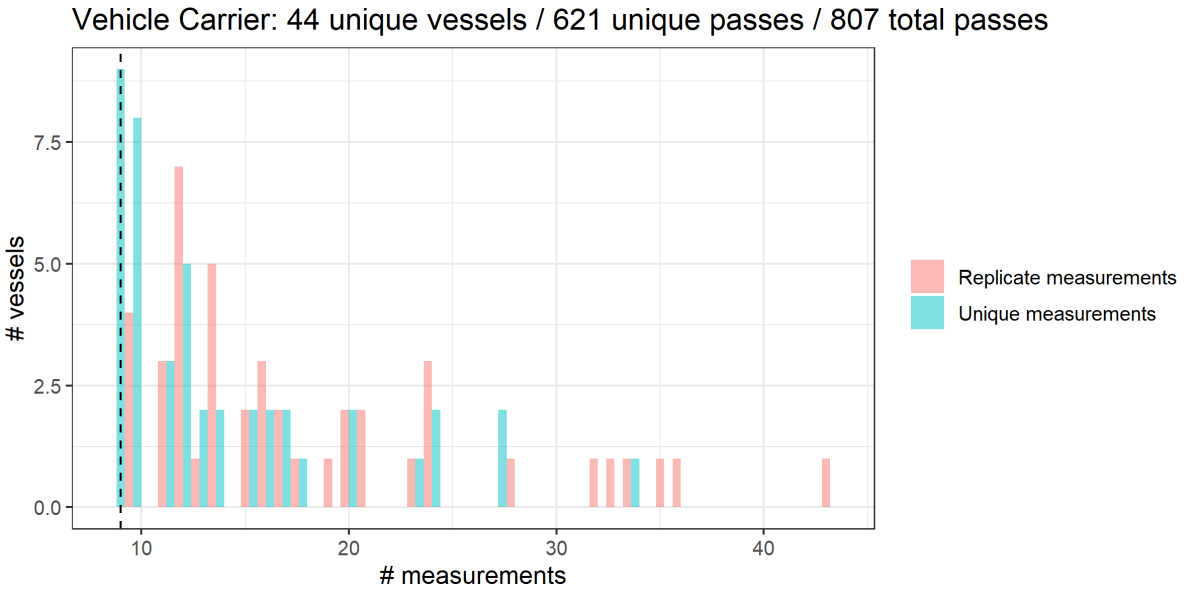

Figure 14. Histogram of the number of unique Vehicle Carriers versus the number of measurements in the data set selected for this study. The vertical dashed line indicates the minimum of 9 unique measurements used for selection of test cases.

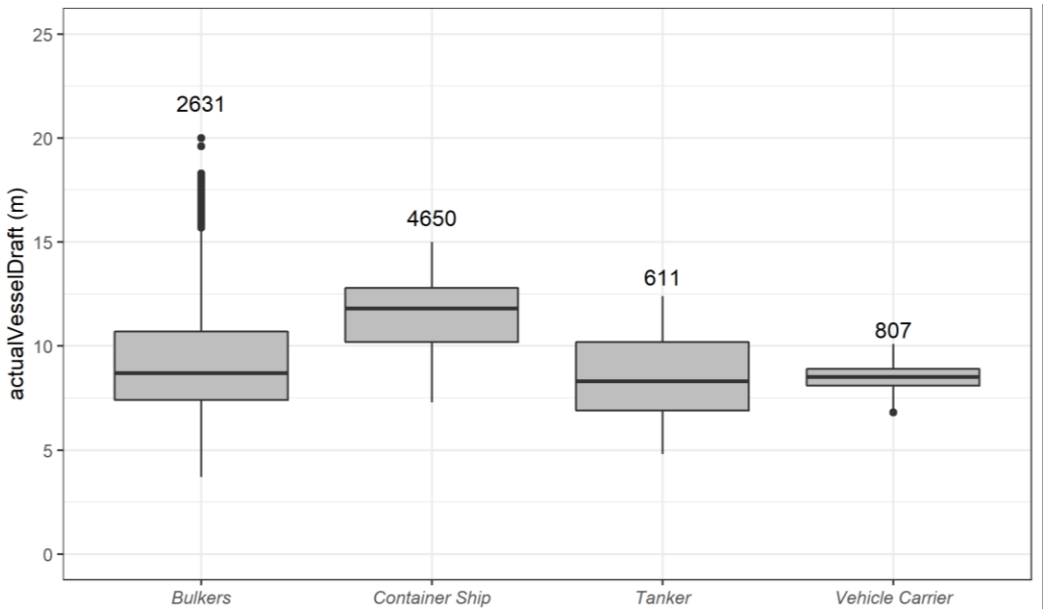

Figure 15. Box-and-whisker plot summarizing actual vessel draft (m) obtained from automatic identification system (AIS) for the data set used in Phase 2 of the Cavitation Inception Speed (CIS) study. Data points shown in the plots were included in the calculated vessel statistics (Table 3).

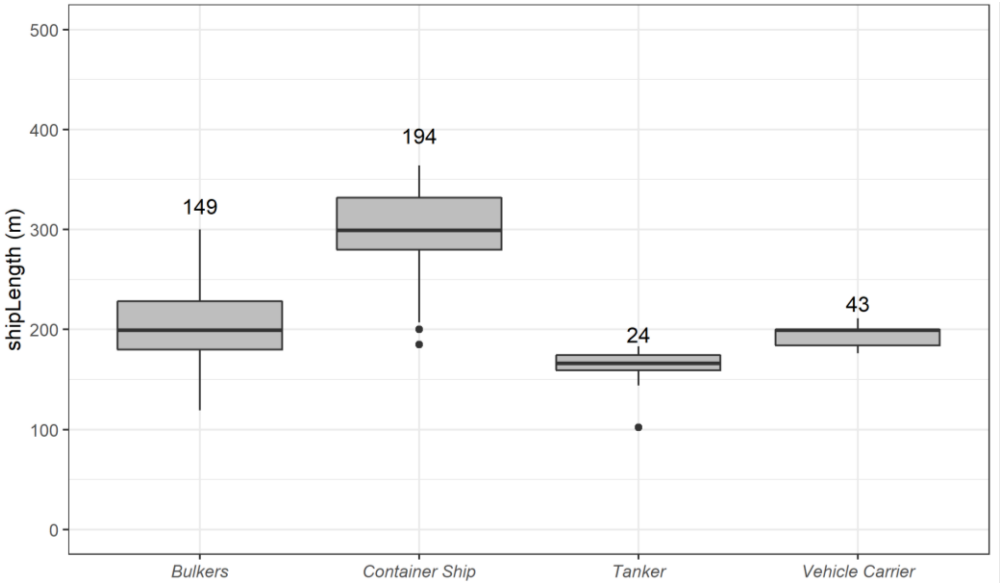

Figure 16. Box-and-whisker plot summarizing overall vessel length (m) for the data set used in Phase 2 of the Cavitation Inception Speed (CIS) study. Data points shown in the plots are included in the calculated vessel statistics (Table 3).

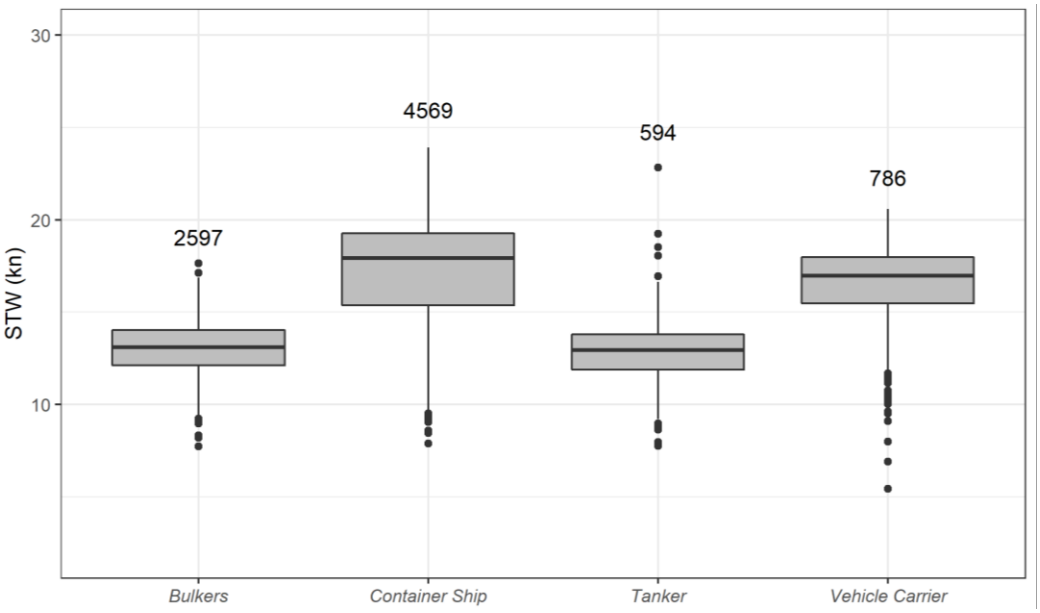

Figure 17. Box-and-whisker plot summarizing speed through water (STW; kn) for the data set used in Phase 2 of the Cavitation Inception Speed (CIS) study. Data points shown in the plots are included in the calculated vessel statistics (Table 3).

Table 3. Summary of statistics (minimum, lower quartile, median, upper quartile, and maximum) per vessel class for the box plots in Figures 15, 16, and 17 corresponding to vessel draft, length, and speed through water (STW), respectively.

Vessel class	# of unique vessels	# of total measurements	Variable	Minimum	Lower quartile	Median	Upper quartile	Maximum
Bulkers	151	2632	Length (m)	119	180	199	228	300
			STW (kn)	7.7	12.1	13.1	14.0	17.6
			Draft (m)	3.7	7.4	8.7	10.7	20.0
Container Ship	195	4656	Length (m)	185	280	299	332	364
			STW (kn)	7.9	15.4	17.9	19.3	23.9
			Draft (m)	7.3	10.2	11.8	12.8	15.0
Tanker	24	611	Length (m)	102	159	166	174	183
			STW (kn)	7.8	11.9	12.9	13.8	22.8
			Draft (m)	4.8	6.9	8.3	10.2	12.4
Vehicle Carrier	44	807	Length (m)	176	184	199	200	211
			STW (kn)	5.5	15.5	17.0	18.0	20.6
			Draft (m)	6.8	8.1	8.5	8.9	10.1

2.6. Evaluation of Descriptors

2.6.1. Descriptor 1: Increase in Low-Frequency Cavitation Hump (20–80 Hz)

The first step in applying Descriptor 1 was to identify the dominant frequency bands contributing to the low-frequency cavitation hump. The frequency range included in this descriptor was adjusted according to the peak frequency range of the cavitation hump for each vessel category (see Figure 18). Based on this analysis, the following frequency bands were used for measuring Descriptor 1 source levels:

- 36–72 Hz for Bulkers and Vehicle Carriers (sum of 40–63 Hz decidecade bands),
- 28–56 Hz for Container Ships (sum of 31–50 Hz decidecade bands), and
- 45–90 Hz for Tankers (sum of 50–80 Hz decidecade bands).

Source levels in these frequency ranges were plotted against STW and fit to the model of Equation 3 to estimate CIS using Descriptor 1.

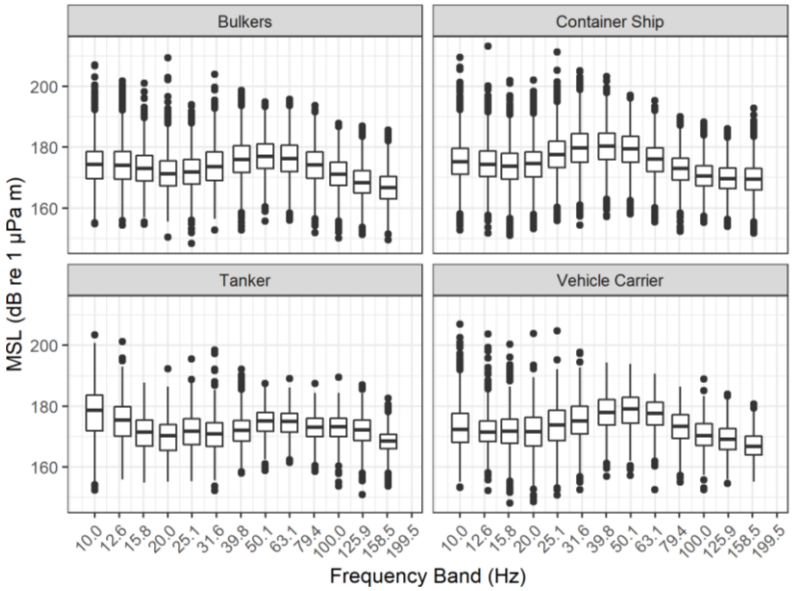

Figure 18. Box-and-whisker plots of decidecade band source levels, by vessel category, used to identify the dominant frequency range of the low-frequency cavitation hump.

Descriptor 1 was evaluated by grouping the URN measurements for each category in two ways:

1. By grouping all vessels in a category and fitting a single set of coefficients (c_1, c_2, and n) to the ensemble of MSL versus STW data. This method yielded a single CIS estimate for each category based on a large number of data points.
2. By considering each vessel separately and fitting a unique set of coefficients (c_1, c_2, and n) to each vessel's MSL versus STW data. This method yielded a single CIS estimate for each vessel based on a smaller number of data points.

Grouping data for all vessels in a category (i.e., method 1) was difficult to apply, in practice, because the NLS algorithm only converged to a statistically significant fit for Container Ships and Vehicle Carriers (Figures 19 and 20). The NLS fit for Bulkers was not statistically significant ($p > 0.05$), and the NLS fit for the Tankers did not converge, suggesting that Equation 3 was not a good fit to the grouped MSL data for this category. By defining CIS as the speed at which the machinery and cavitation noise intersect, the NLS fits suggested CIS values of 9 kn for Vehicle Carriers, and 10.3 kn for Container Ships. These single-number estimates represented the best fit to the full data ensemble for each category, but they were generally lower than the single-vessel estimates (below) and likely less reliable.

The definition of CIS as the crossing point between machinery and cavitation noise components is somewhat arbitrary: a comprehensive evaluation of cavitation noise by an expert sonar operator could eventually reveal that well-developed cavitation is audible/detectable when the cavitation model is a few decibels higher than the machinery noise.

Visual inspection of Figures 19 and 20 may seem to suggest that the machinery noise component is underestimated since it would be tempting to increase C_1 (i.e., shift the blue line upwards) to improve the alignment of the model to some of the data points at the lower speeds. However, careful examination of the MSE reveals that any changes in C_1 (keeping all other parameters constant) would worsen the fit of the NLS model (Equation 3) with the net effect of increasing the MSE, as shown in Figure 21.

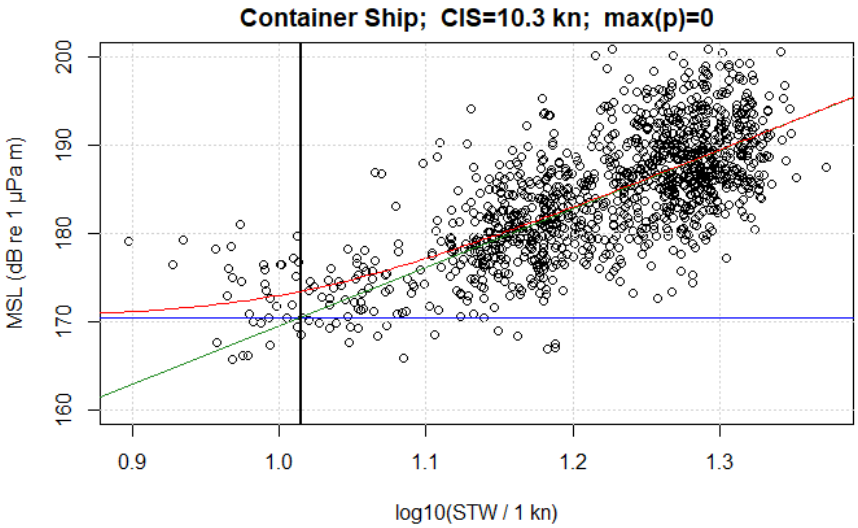

Figure 19. Broadband monopole source level (MSL) hump (28–56 Hz) for Container Ships versus the logarithm of speed. The blue and green lines represent the non-linear least squares (NLS) fit for the machinery and cavitation models, respectively. The red line represents the summation of the two models. The solid vertical line indicates the speed at which the machinery and cavitation noise model intersect (10.3 kn STW).

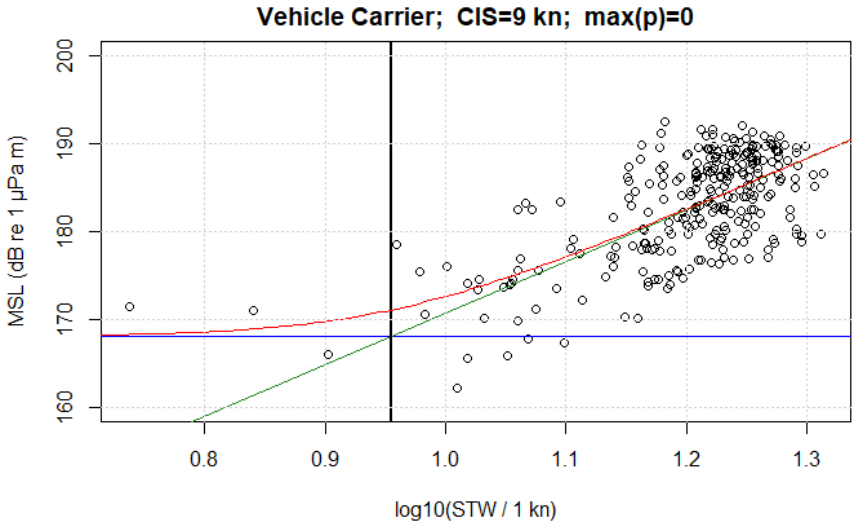

Figure 20. Broadband monopole source level (MSL) hump (36–72 Hz) for Vehicle Carrier versus the logarithm of speed. The blue and green lines represent the non-linear least squares (NLS) fit for the machinery and cavitation models, respectively. The red line represents the summation of the two models. The solid vertical line indicates the speed at which the machinery and cavitation noise model intersect (9 kn STW).

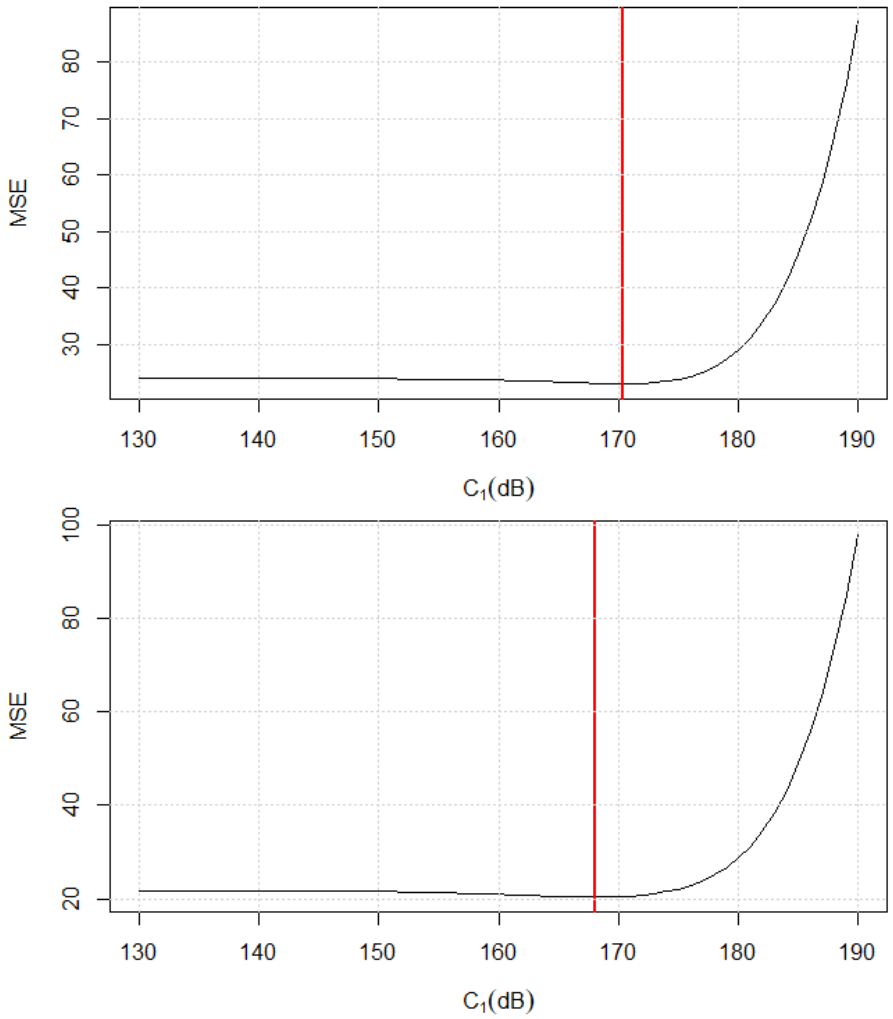

Figure 21. Investigation of the variation of the mean square error (MSE) with the machinery noise (C_1) parameter for (top) Container Ship and (bottom) Vehicle Carrier. To obtain these plots, the non-linear least squares fit from Figures 19 and 20 (Container Ship and Vehicle carrier, respectively) and the MSE were re-computed by varying C_1. The vertical red line indicates the minimum MSE, which matches the C_1 estimated by the non-linear least squares (NLS) algorithm.

Applying the NLS fit to individual vessels (i.e., method 2) proved to be more successful than applying the NLS fit to the entire data ensemble for each category. The advantage of applying the fit to each vessel is that it yields multiple estimates of the CIS (i.e., one per vessel), from which statistical properties of the estimate (such as its mean and standard deviation) can be quantified. The disadvantage is that the number of data points available to constrain the NLS fit is significantly reduced when dealing with individual vessels.

The NLS algorithm provided convergent estimates for 94 of the 191 vessels that were evaluated. Figure 22 shows an example of a convergent NLS fit for a single vessel, which indicates a CIS of 12.2 kn. For the remaining 97 cases where the NLS fit algorithm did not converge, Equation 3 was not a good fit to the data. This generally occurred in cases where the SL versus STW data exhibited a linear trend with no evidence of an inflection point at lower speed.

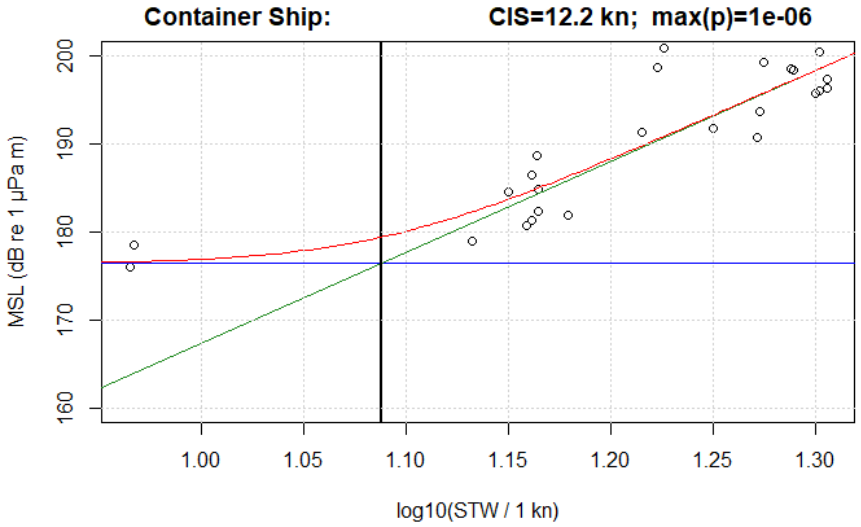

Figure 22. Broadband monopole source level (MSL) hump (28–56 Hz) for a single Container Ship versus the logarithm of speed. The blue and green lines represent the non-linear least squares (NLS) fit for the machinery and cavitation models, respectively. The red line represents the summation of the two models. The solid vertical line indicates the speed at which the machinery and cavitation noise model intersect (12.2 kn STW).

Even when the NLS algorithm converged, the resulting fit coefficients were not always statistically significant. Figure 23 shows scatter plots of the p-value of the estimated values versus the model parameters C_1, C_2, and n for each vessel. Only p-values < 0.05 are considered statistically significant and therefore models with maximum p-values greater than this threshold were excluded when computing the mean and standard deviation CIS. Removing cases with high p-value left 41 vessels with statistically significant CIS estimates as shown in Figure 24 and summarized in Table 4. Based on the percent of vessels that yielded a CIS estimate, this descriptor was most successful when applied to vessels with a greater speed range (i.e., Container Ships and Vehicle Carriers), and less successful when applied to vessels with a smaller speed range (i.e., Tankers and Bulkers).

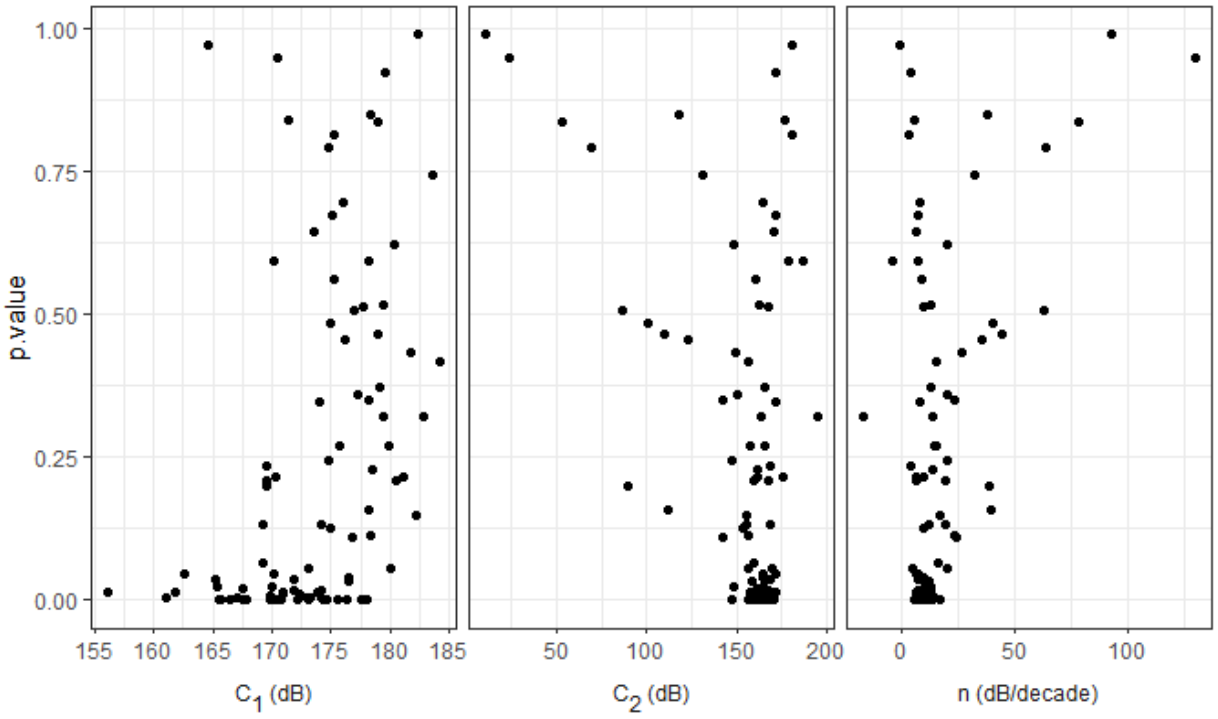

Figure 23. P-value of the non-linear least squares (NLS) fit parameters c_1, c_2, and n.

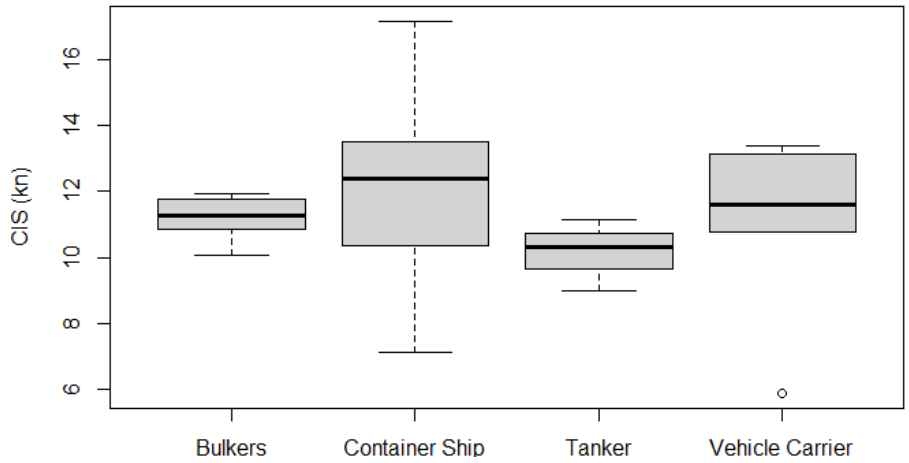

Figure 24. Box-and-whisker plot summarizing the statistics of the per-vessel estimates of Cavitation Inception Speed (CIS) obtained using Descriptor 1.

Table 4. Summary (mean, standard deviation, # of vessels) of statistically significant Cavitation Inception Speed (CIS) estimates, obtained using Descriptor 1 (see Figure 24). Statistics were estimated using only estimates with $p \leq 5$ %. The percent of vessels used in the estimate is computed from the total number of vessels analyzed.

Category	# vessels analyzed	# vessels with CIS estimate	# vessels with CIS estimate ($p \leq 5$ %)	Percent of vessels with CIS estimate ($p \leq 5$ %)	Mean CIS (kn)	Standard deviation (kn)
Bulkers	117	53	7	6	11.2	0.71
Container Ships	47	28	26	55	12.0	2.31
Tankers	12	4	3	25	10.1	1.08
Vehicle Carriers	15	9	5	33	11.0	3.03

2.6.2. Descriptor 2: Number of Tonals Below 100 Hz

Figure 25 shows the results of an early exploration of Descriptor 2, in which we computed the mean tone count per decidecade band, parameterized by vessel category (columns), tonal detector threshold (rows), and vessel speed (colour). For all vessel categories except Tanker, the tonal count in most frequency bands tends to be higher at lower speeds. The same pattern was observed for all detector thresholds, but the overall tone count decreased at detector threshold increased. This is particularly clear for the Container Ship and Vehicle Carrier categories.

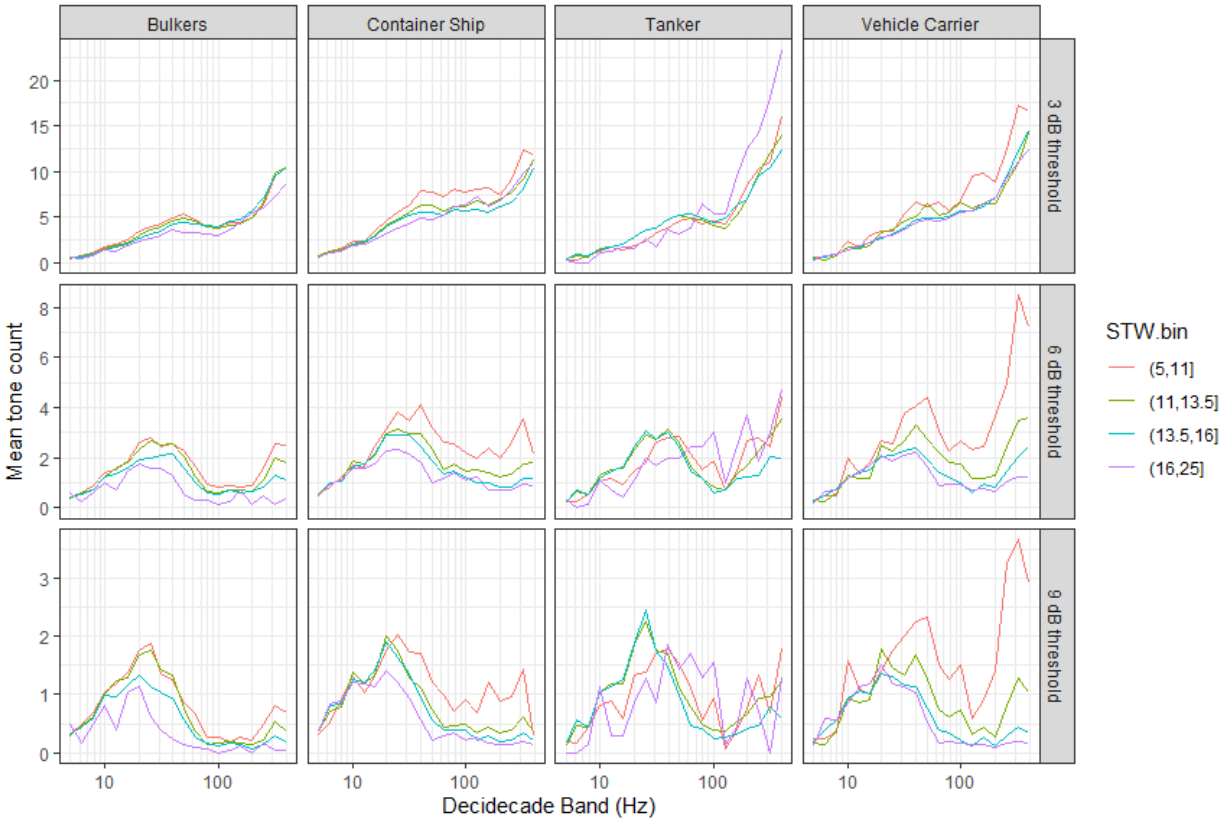

Figure 25. Mean tone count as a function of frequency, obtained by binning the data in coarse speed bins (colour coded). For Bulkers, Container Ships, and Vehicle Carriers, there is a tendency of high tonal counts at lower speeds.

The results in Figure 25 served as proof of concept to refine a frequency band and detector threshold. Figure 26 shows statistics of the 10–100 Hz tone count as a function of STW (1 kn bins) for the 6 dB detector threshold, which yielded the best results compared to other frequency and threshold choices. In all cases except for Tankers, the mean count is higher at lower speeds, as expected from the descriptor's hypothesis. The transition from high to low tonal count is smooth for Bulkers, so it is difficult to identify a particular CIS. For the Container Ship and Vehicle Carrier categories, a distinct transition in the 10–100 Hz tone count appears to occur above 12 kn.

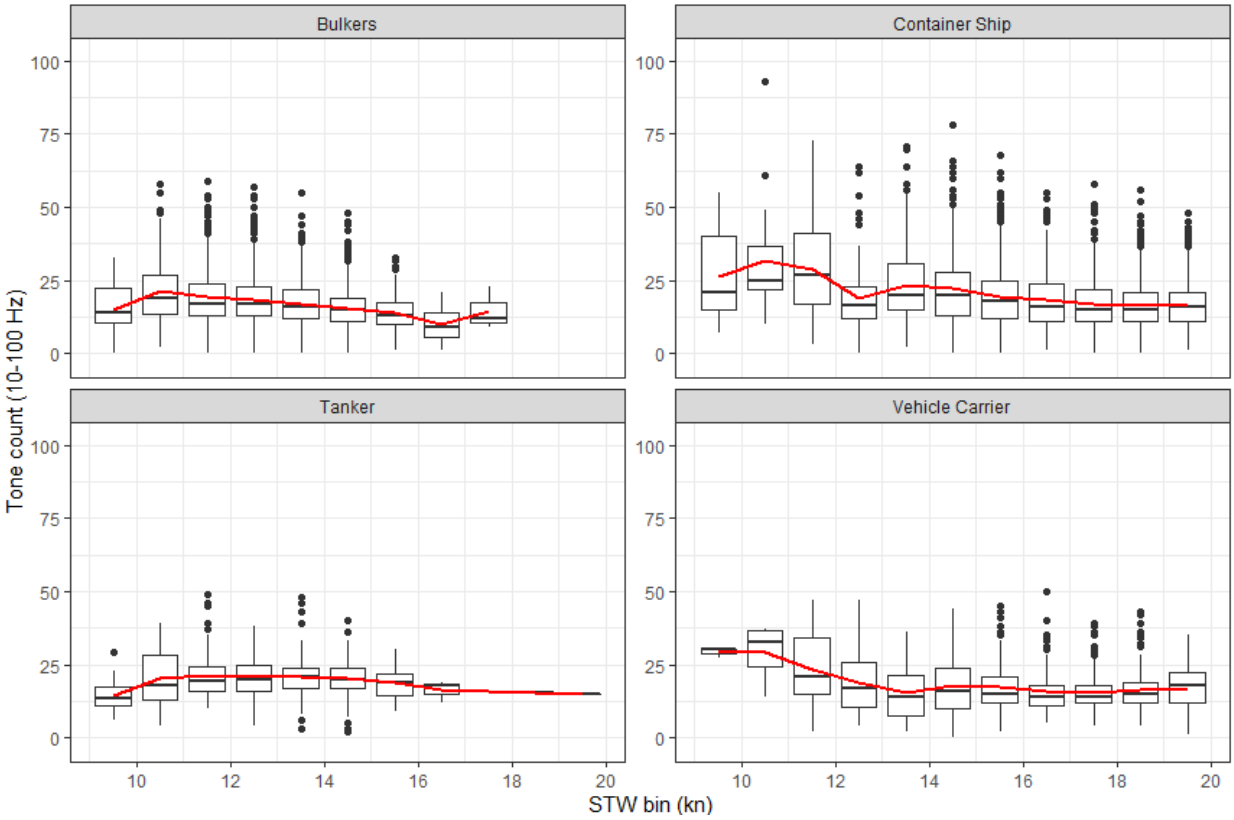

Figure 26. Statistics of the tone count within 10–100 Hz as a function of speed through water (STW; 1 kn bins) for the 6 dB detector threshold. The superimposed red line represents the mean count.

2.6.3. Descriptor 3: Spectral Slope

Figure 27 shows an example of the spectral slope between 0.1–20 kHz as a function of speed, for all Vehicle Carriers. For many vessels, there is a tendency towards more negative slope values at lower speeds, which indicates a flattening of the spectrum with increasing speed. In some panels, there are no data at low speeds (i.e., <10 kn), which makes it difficult to verify whether this tendency is widespread. However, for most vessels with low-speed data, the slopes at the lowest speed correspond to the most negative values, consistent with the descriptor's hypothesis (see Section 2.3.3).

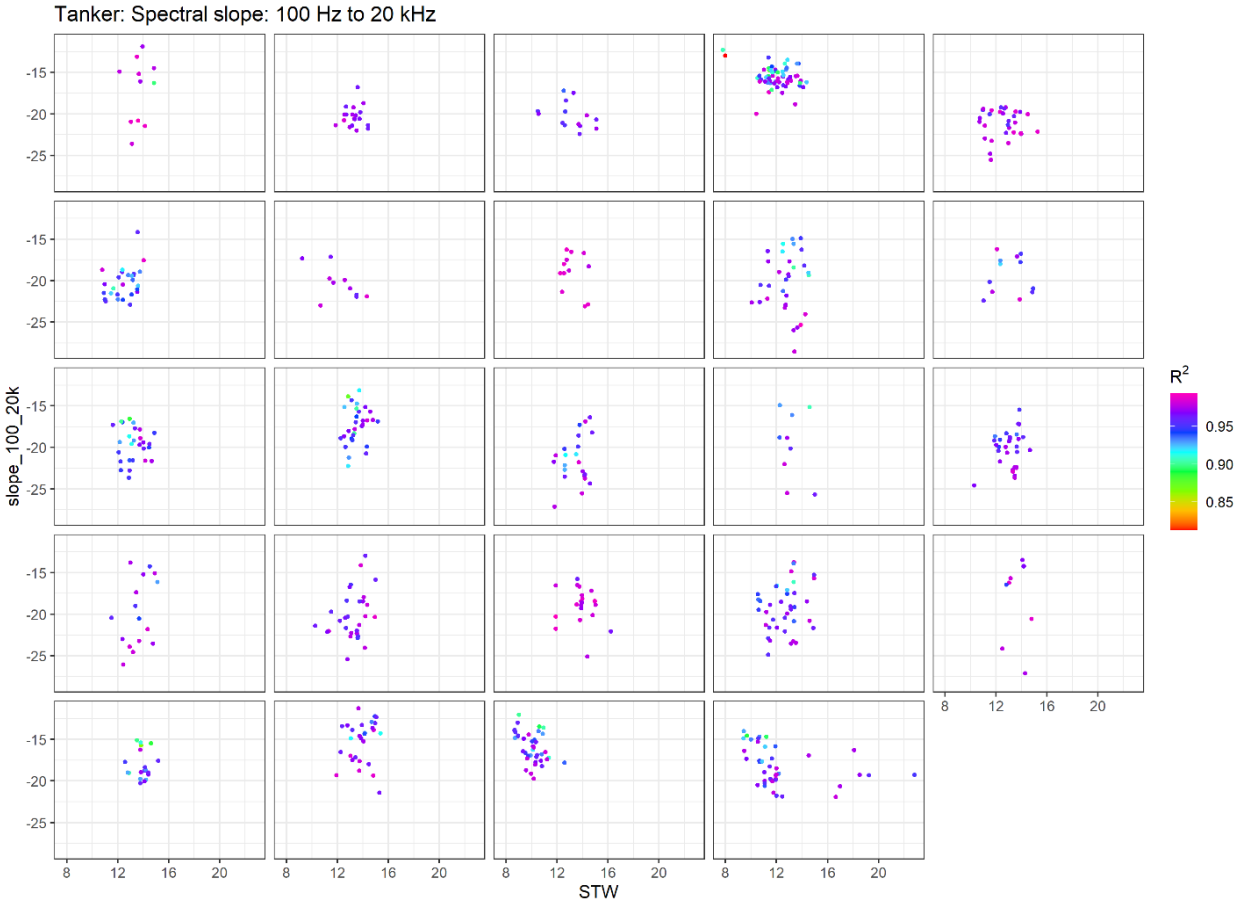

Figure 27. Spectral slope from 0.1–20 kHz versus vessel speed (kn) for all 44 Vehicle Carriers. The color scale shows the coefficient of determination (R^2) of the estimated slope for each underwater radiated noise (URN) measurement.

Figure 28 gathers the estimated slope between 0.1–20 kHz for all data and categories versus STW. In all cases, the coefficients of determination (R^2) of the data points were very high, indicating a strong degree of confidence in the slope estimates provided by the descriptor. The solid blue line is a linear fit to the data, and it shows the expected trend for Container Ship and Vehicle Carrier categories, although with substantial data scatter around the fit. Such a large amount of scatter occurs because, as shown in Figure 27, spectral slope values appear to be distinct for each individual vessel. Descriptor 3 performed poorly for Bulkers and Tankers. For Bulkers, there is no clear evidence of a trend. For Tankers, the trend is opposite to the proposed hypothesis.

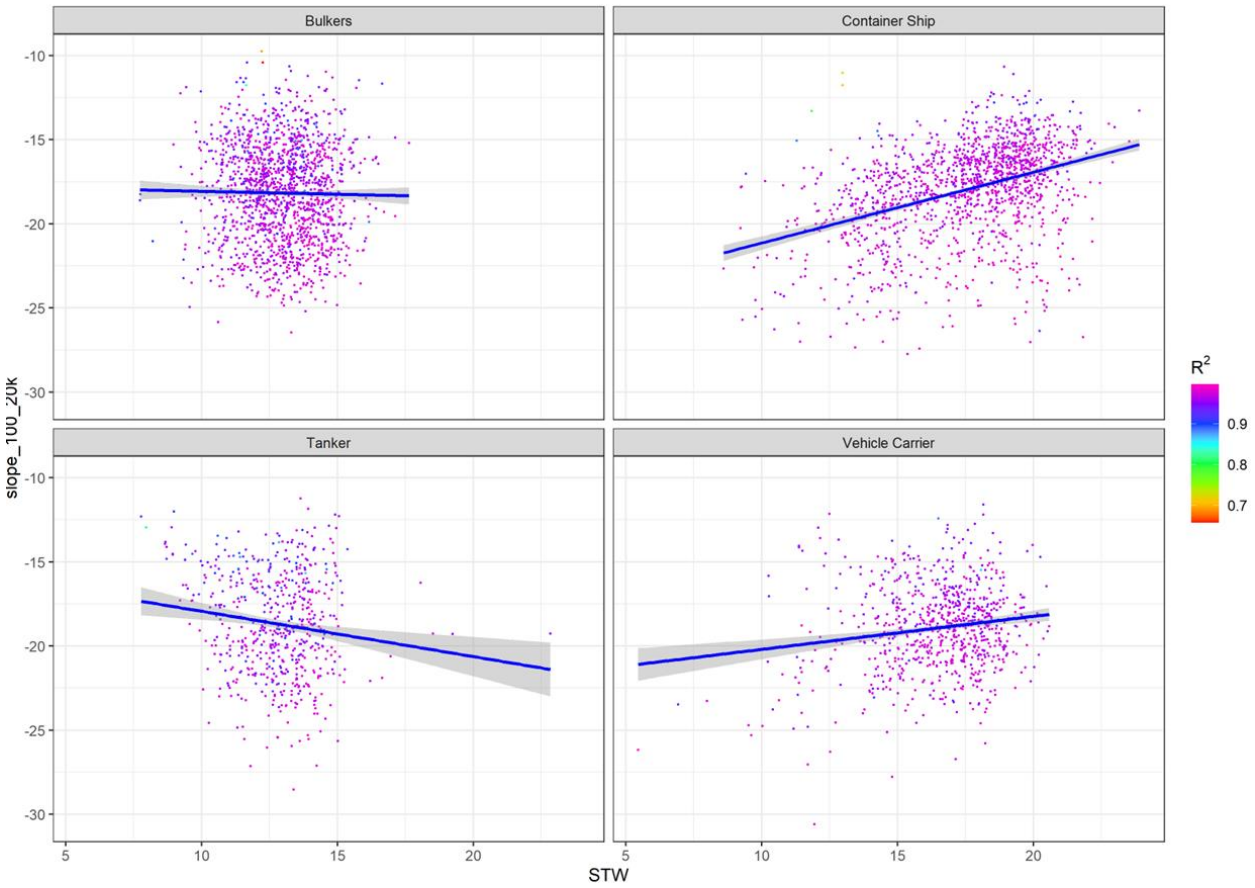

Figure 28. Spectral slope from 0.1–20 kHz versus vessel speed. The color scale shows the coefficient of determination (R^2) of the estimated slope for each underwater radiated noise (URN) measurement. The blue lines represent linear fits to the data.

2.6.4. Descriptor 4: Factor X of URN Increase Relative to Speed

While applying Descriptor 4 to the data, it was found that the local slope X estimator (see Section 2.3.4) yielded results with high variability. To reduce this variability, we binned the data by STW and took the median MSL within each bin. An example of the resulting smoothed data is shown as a solid blue line in Figure 29 for container ships. Despite the reduction in variability, computing the X slope using the binned values (the blue line) still resulted in significant variability without a clear trend of increasing X as a function of speed (see Figure 30). For this reason, this descriptor was not pursued further.

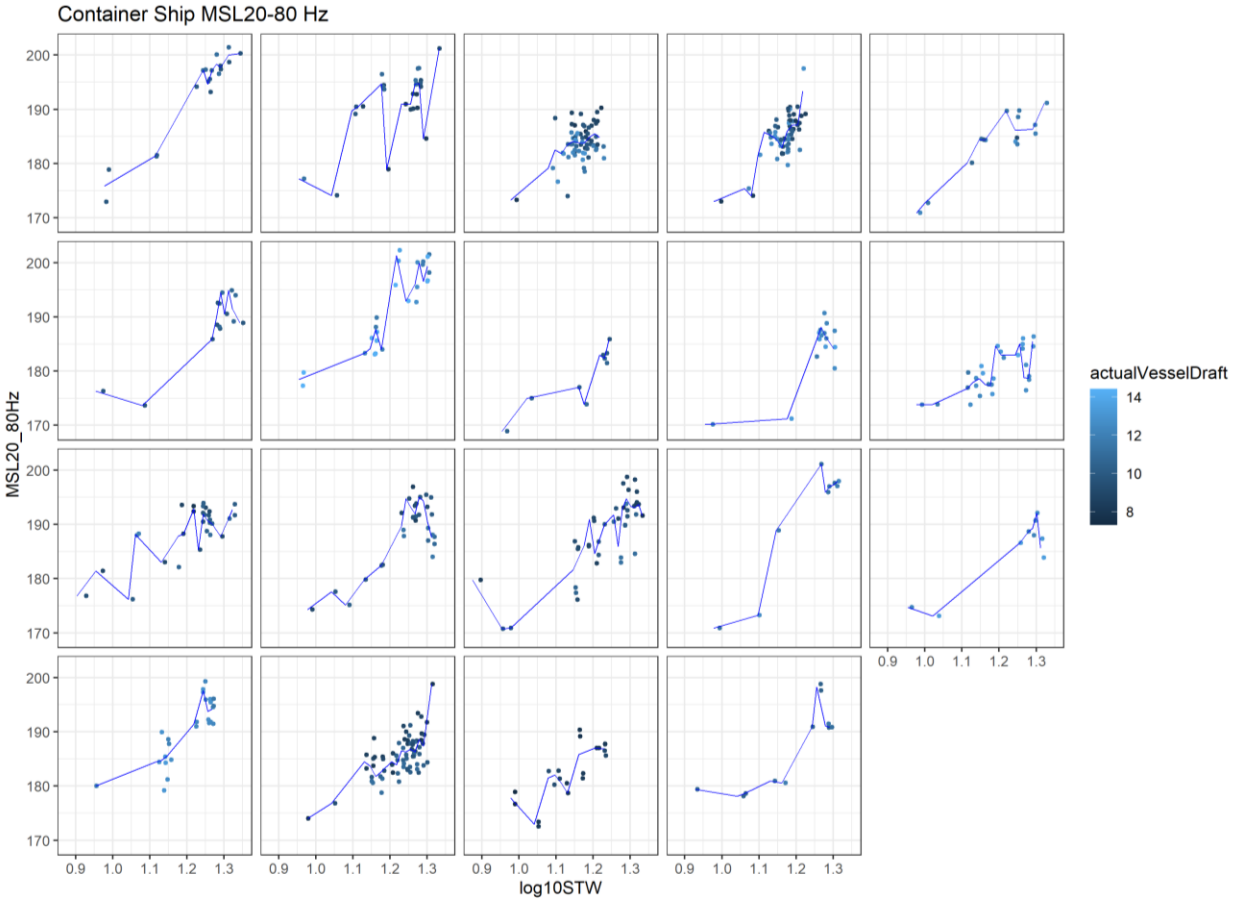

Figure 29. Data smoothing performed prior to the computation of the X slope factor as an attempt to reduce variability in the estimated local slope.

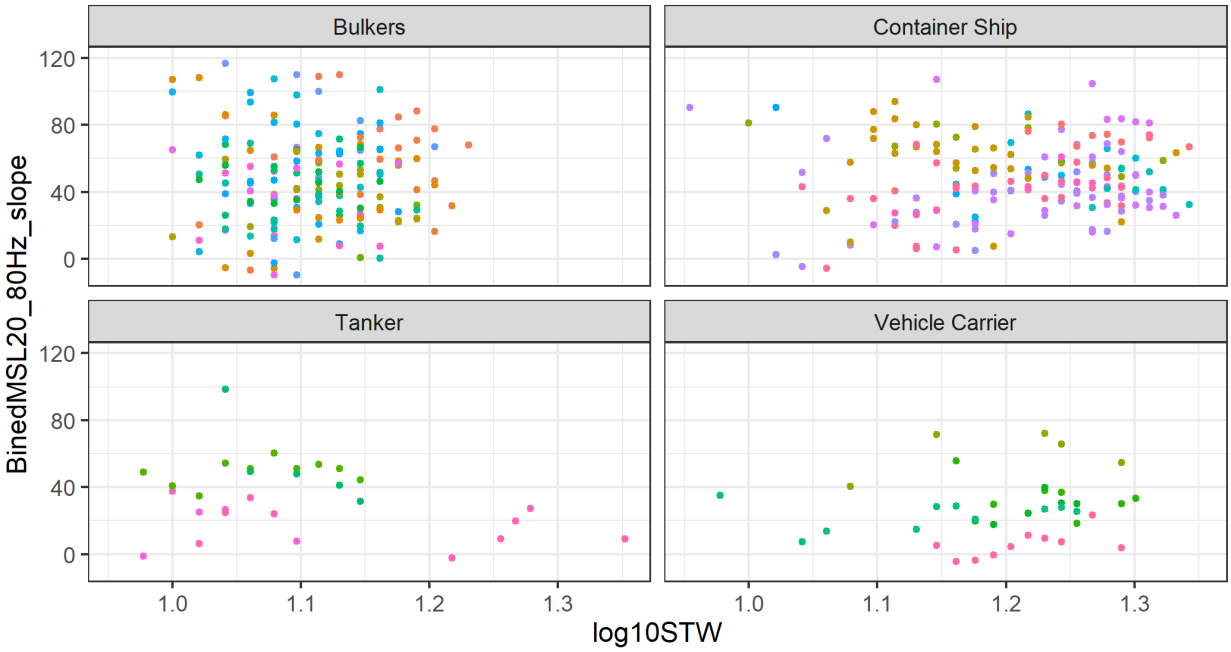

Figure 30. Local slope X estimated for all vessels. Colours indicate different vessels.

2.6.5. Descriptor 5: Confidence of Dual-band RPM Estimator

As mentioned in Section 2.3.5, the RPM estimator analyses two bands and yields a single RPM estimate based on which of the band estimators yields the highest confidence. This RPM dual estimator was run for all test cases in the ECHO database, which archives the RPM estimate with the highest confidence, the confidence factor (either CF_{LB} and CF_D), and a DEMON flag to indicate whether the estimate and confidence factor came from the DEMON band or the LB band estimators, as shown in Table 5. From Table 5, we can separate the results as follows: For DEMON flag=1,2, and 5, the confidence refers to the LB estimator. For DEMON flag=3,4, the confidence refers to the DEMON estimator.

Table 5. Interpretation of the Detection of Envelope MOdulation on Noise (DEMON) flag from JASCO'S dual band RPM estimator.

Condition	Valid LB?	Valid DEMON?	CF	DEMON flag
Both estimators agree on RPM	Yes	Yes	$max(CF_D, CF_{LB})$	0
$RPM_D = 2\ RPM_{LB}$	Yes	No	CF_{LB}	1
$CF_D < CF_{LB}$	Yes	Yes	CF_{LB}	2
$CF_D > CF_{LB}$	Yes	Yes	CF_D	3
Only DEMON estimator valid	No	Yes	CF_D	4
Only LB estimator valid	Yes	No	CF_{LB}	5

In this investigation, we tested whether a trend between the vessel speed (STW) and the RPM confidence factor could be used to detect cavitation. The expectation was to observe high DEMON confidence for cases with strong cavitation (i.e., a positive linear trend in Figure 32), and also high LB confidence in cases of low cavitation (i.e., a negative linear trend in Figure 31). In addition, for cases with mild cavitation, the expectation was to see both LB and DEMON estimators perform with high confidence (Figure 33). Such trends were not observed, so it was decided not to continue pursuing this descriptor as currently computed. A recommendation would be to modify the confidence factor to specifically quantify the quality of the LB and DEMON spectrum (as opposed to also include the quality of the RPM estimate), but such implementation was beyond the scope of this investigation.

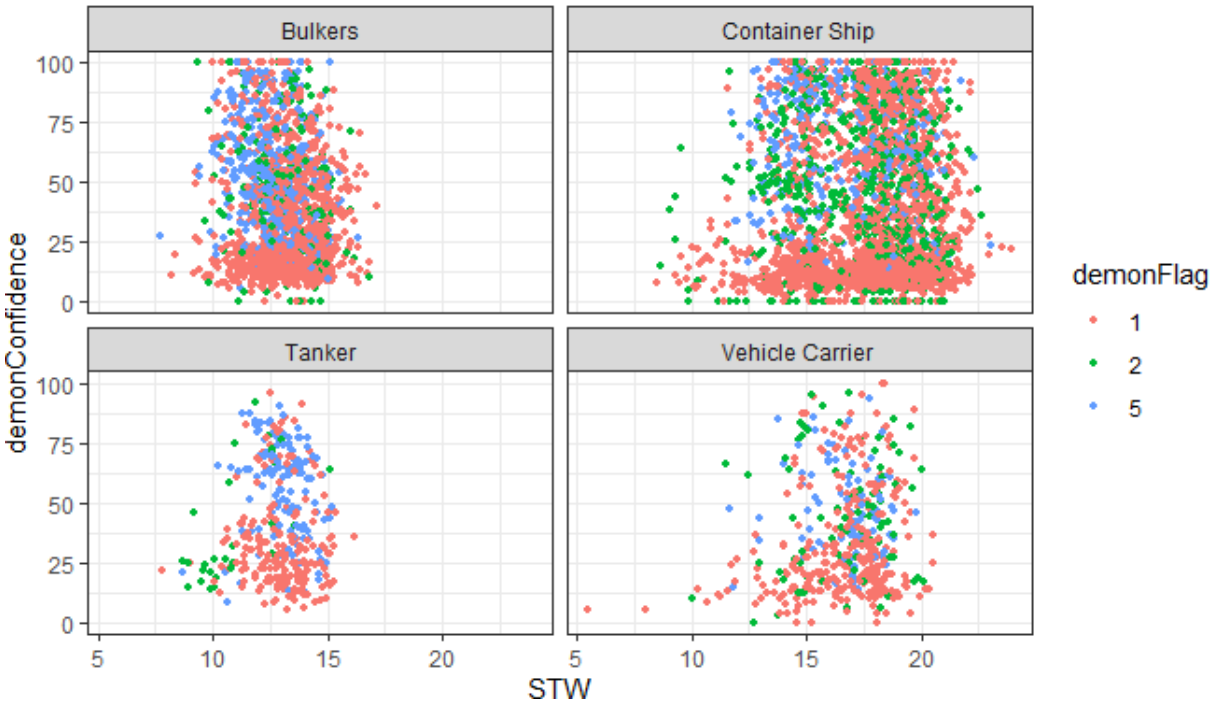

Figure 31. Confidence factor of JASCO's dual band RPM estimator, corresponding to the LB estimator (DEMON flag=1,2, and 5; see Table 5).

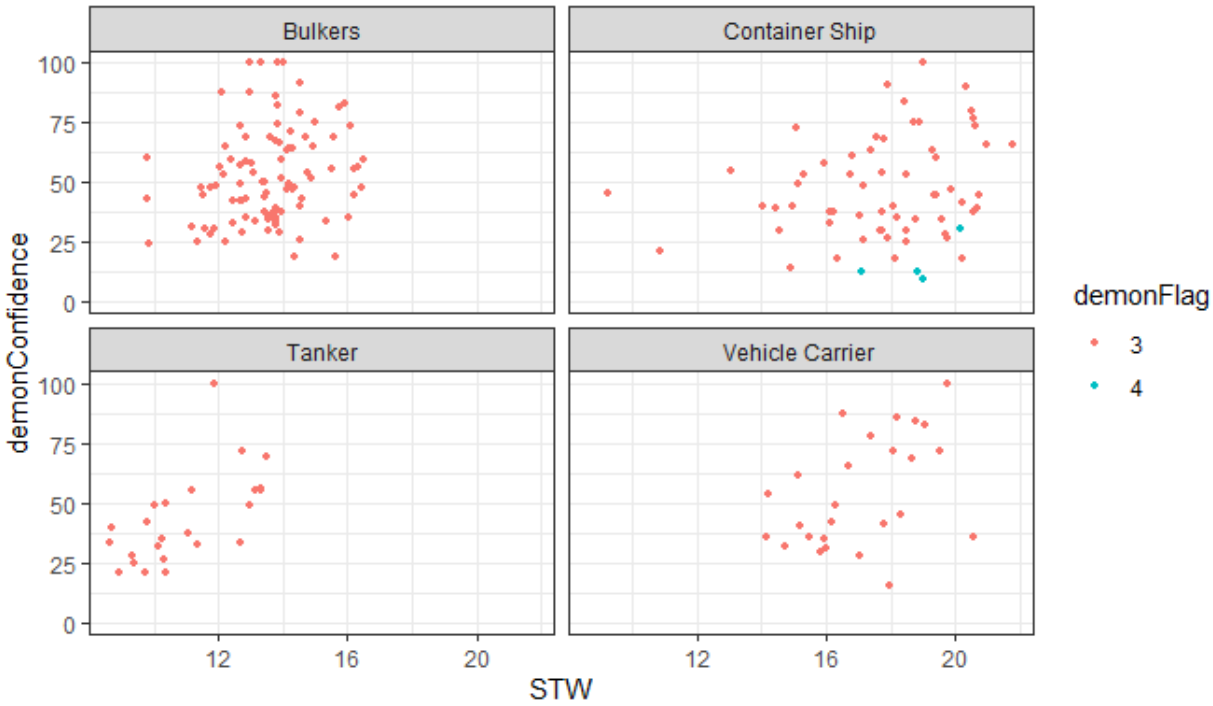

Figure 32. Confidence factor of JASCO's dual band RPM estimator, corresponding to the DEMON estimator (DEMON flag=3 and 4; see Table 5).

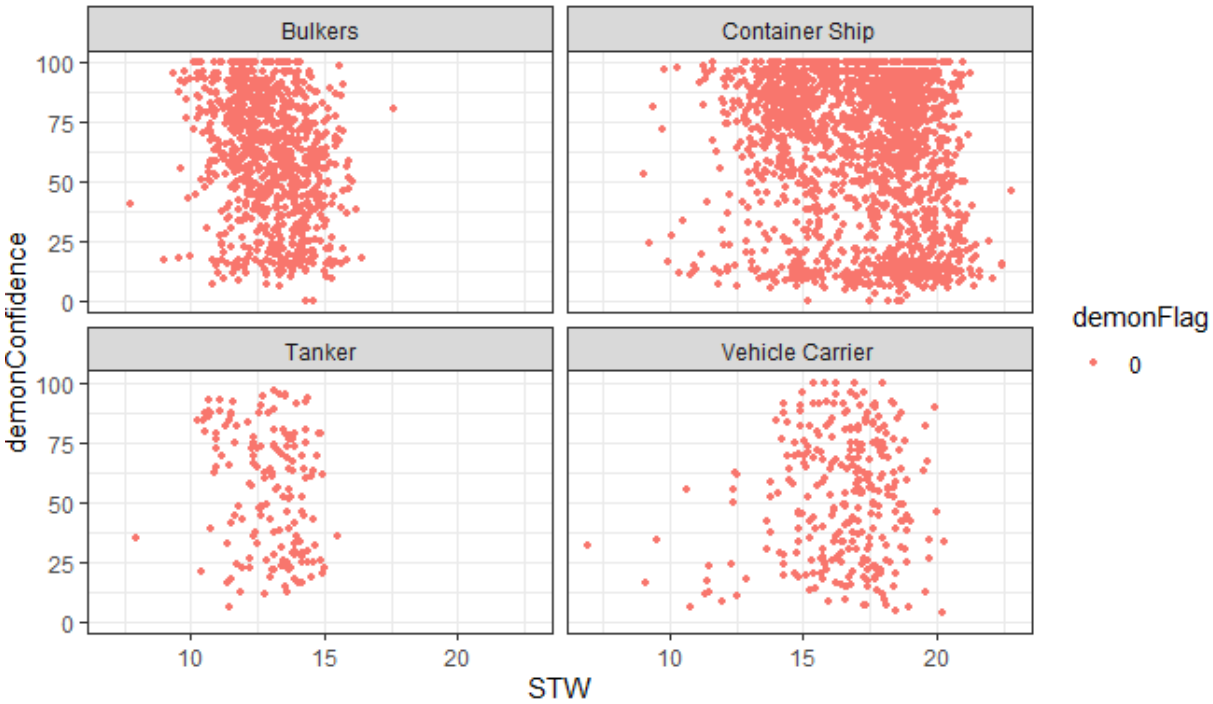

Figure 33. Confidence factor of JASCO's dual band RPM estimator, corresponding to cases in which LB and DEMON estimators obtained the same RPM (DEMON flag=0; see Table 5).

2.7. Manual Validation

To investigate cavitation inception, manual analysis of 30 measurements from 10 vessels was performed to identify typical cavitation noise and the frequency range affected by it. The vessels were selected to have measurements corresponding to low, mid, and high STW (Figure 34), since this would permit analysis of their spectral and cavitation features in three operational speed regimes.

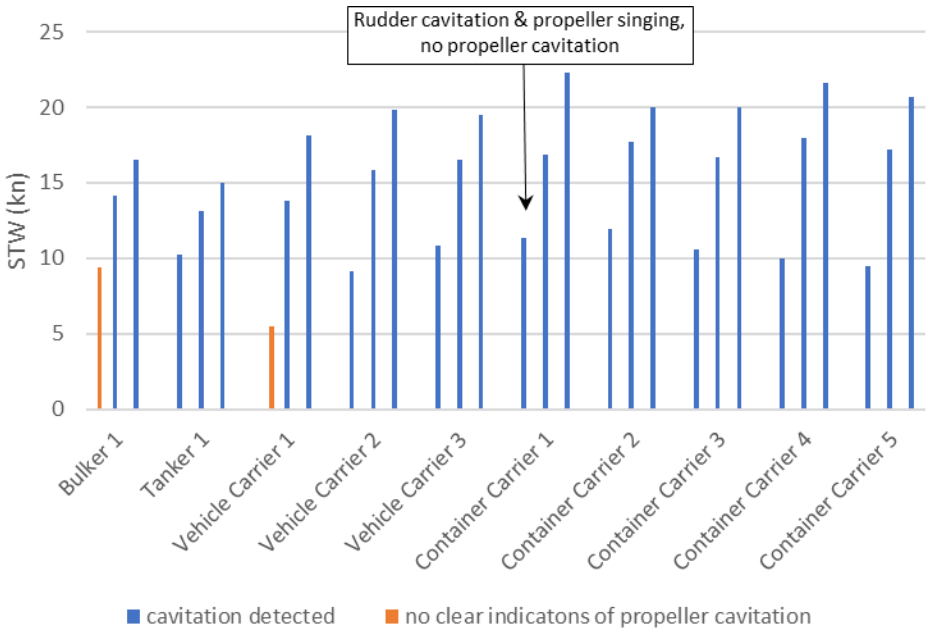

Figure 34. Overview of measurements considered in manual cavitation analysis: low, mid, and high speed measurements were selected for 10 vessels, for a total of 30 measurements.

The three measurements corresponding to each individual vessel are expected to exhibit variability not only because of the different speed but also because of the following factors:

- Differences in draft, which have significant impact on ship drag and on hydrostatic pressure on the propeller, both of which affect occurrence of cavitation.
- The time elapsed between measurements, which can affect acoustic characteristics due to significant amounts of biofouling that can accumulate over time and affect drag and hydrodynamics of the propeller, and due to potential ship repairs/maintenance between measurements.

As an example, Figure 35 illustrates the potential impact of draft on the noise spectral characteristics: above 630 Hz, the source level at 14.4 kn STW with 11.8 m draft is up to 10 dB higher compared to the measurement at 16.5 kn STW with 7.6 m draft. Additionally, a broadband hump around 400 Hz is only present for the two measured conditions at shallow draft. This hump is not observed in the heavily loaded condition at 11.8 m draft, which is a hint that the extent of cavitation is not only dependent on draft but also on the type of cavitation.

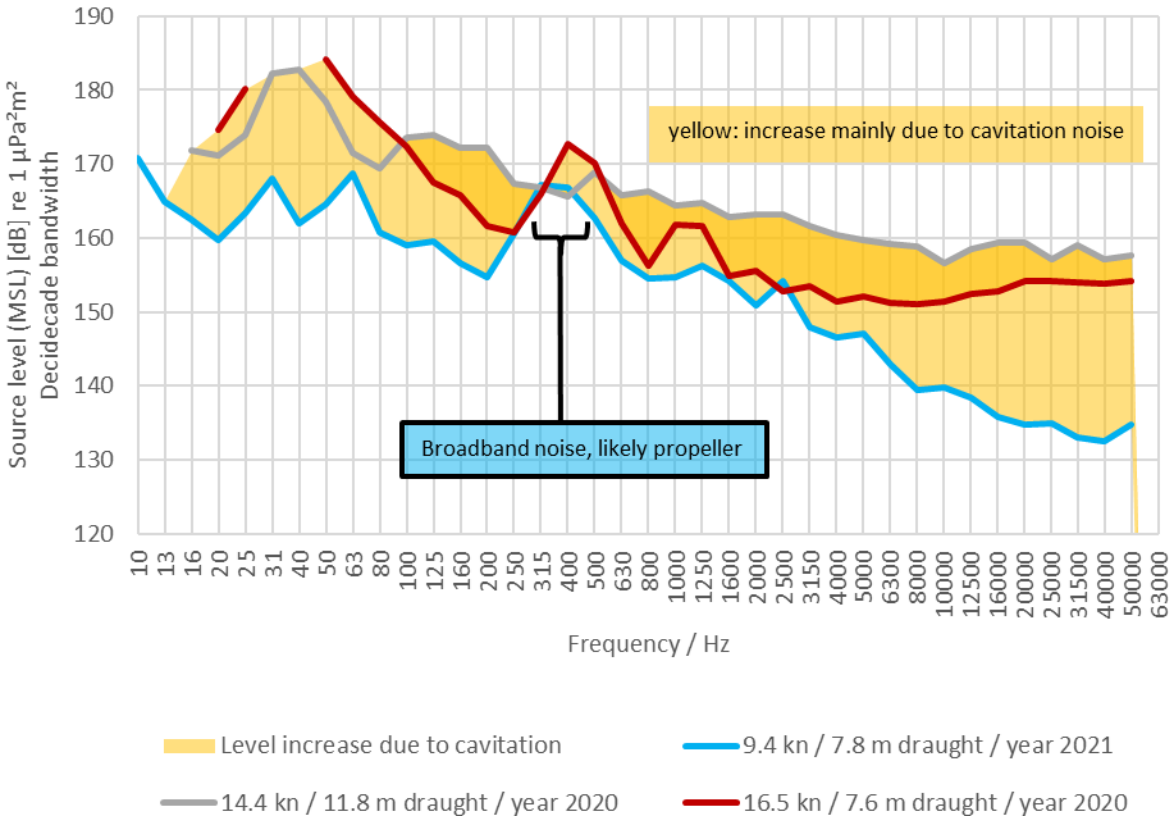

Figure 35. Decidecade source level for 3 measurements corresponding to Bulker 1. The broadband hump around 400 Hz, attributed to cavitation with high probability, is observed at shallow draft while it is not present when the ship is heavily loaded.

An example to illustrate spectral variability potentially due to the amount of time between the measurements is shown in Figure 36, which compares measurement results 4 years apart (2017 and 2021). Ignoring the contribution of propeller singing, the source levels above 1.25 kHz are very similar for measurements at 11.3 kn STW with 12.6 m draft and 16.9 kn STW with 13.7 m draft. Within this range of draft variations, an increase of speed would typically show significant impact on source levels as has been shown in three phases of vessel correlation studies (MacGillivray et al. 2020a, MacGillivray et al. 2020b). The small increase of source level in this case can possibly be explained by technical modifications in between the measurements. However, there was no data available to validate this assumption.

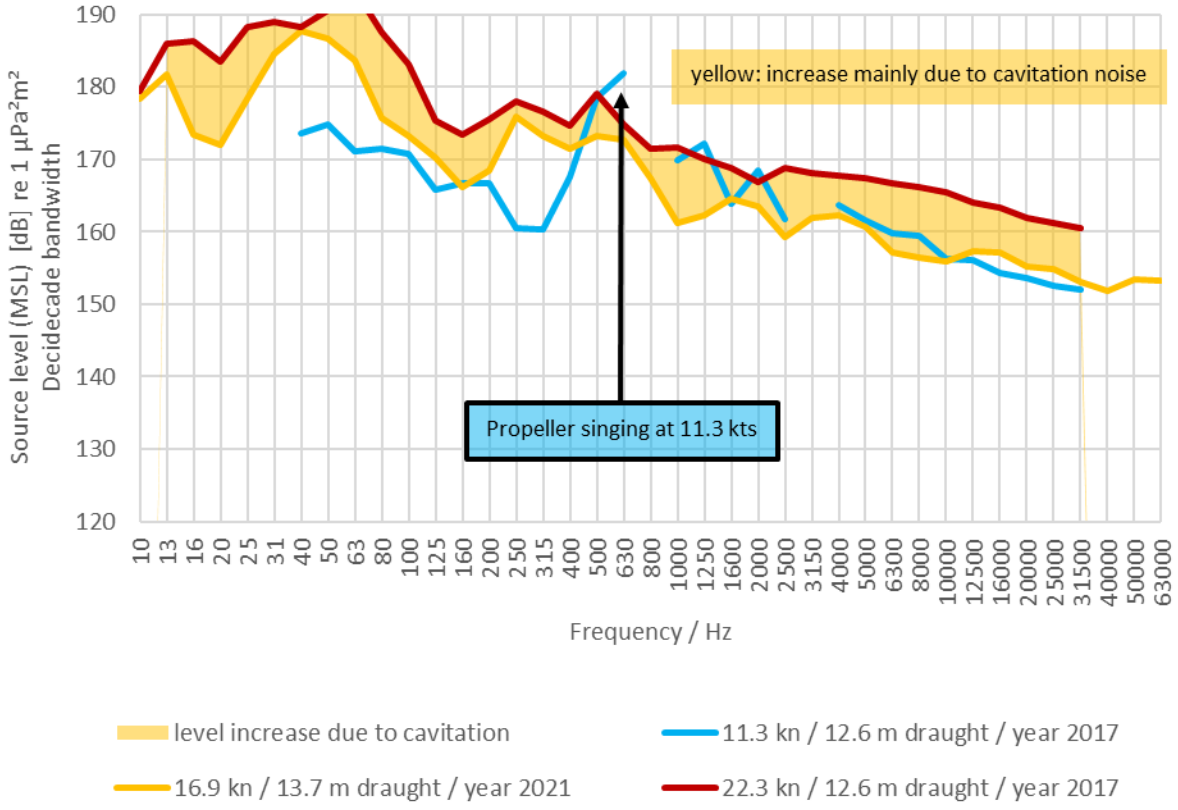

Figure 36. Decidecade source level for 3 measurements corresponding to Container Carrier 1. Missing MSL data correspond to bands rejected due to high background noise, as identified by ShipSound in accordance with the ISO 17208-1 URN standard measurement procedure.

Table 6 shows the results of audio analysis of the 30 measurements to detect the presence of cavitation. In only 3 out of the total 30 recordings was propeller cavitation absent or undetectable (with suspected rudder cavitation present in 1 of those 3 cases). The corresponding source level spectra are summarized in Figure 37 to provide examples of typical levels without propeller cavitation present:

- Vehicle Carrier 1 at 5.5 knots, for which noise was fully dominated by two-stroke main engine.
- Vehicle Carrier 2 at 9.1 knots, with evaluation complicated by overlay of cetacean clicks and vocalizations.
- Container Carrier 1 at 11.3 knots, which exhibits features of propeller singing that typically only occur in absence of cavitation.

For these three cases, further reduction of ship speed would likely lead to marginal reductions of source levels.

This manual analysis deals with an ensemble of ships that is comparable with the larger data set investigated by automated analysis. For measurements without acoustically detectable propeller cavitation, the dominant noise source is the two-stroke engine. As a side result it was found that only very few ships contained detectable contribution of auxiliary machinery. These were mostly vehicle carriers that are typically optimized for height of the vehicle decks, leading to flat engine rooms where all machinery is mounted on the lowest deck. Compared to arrangements with generator engines mounted on tween decks, this arrangement leads to increased underwater noise radiation.

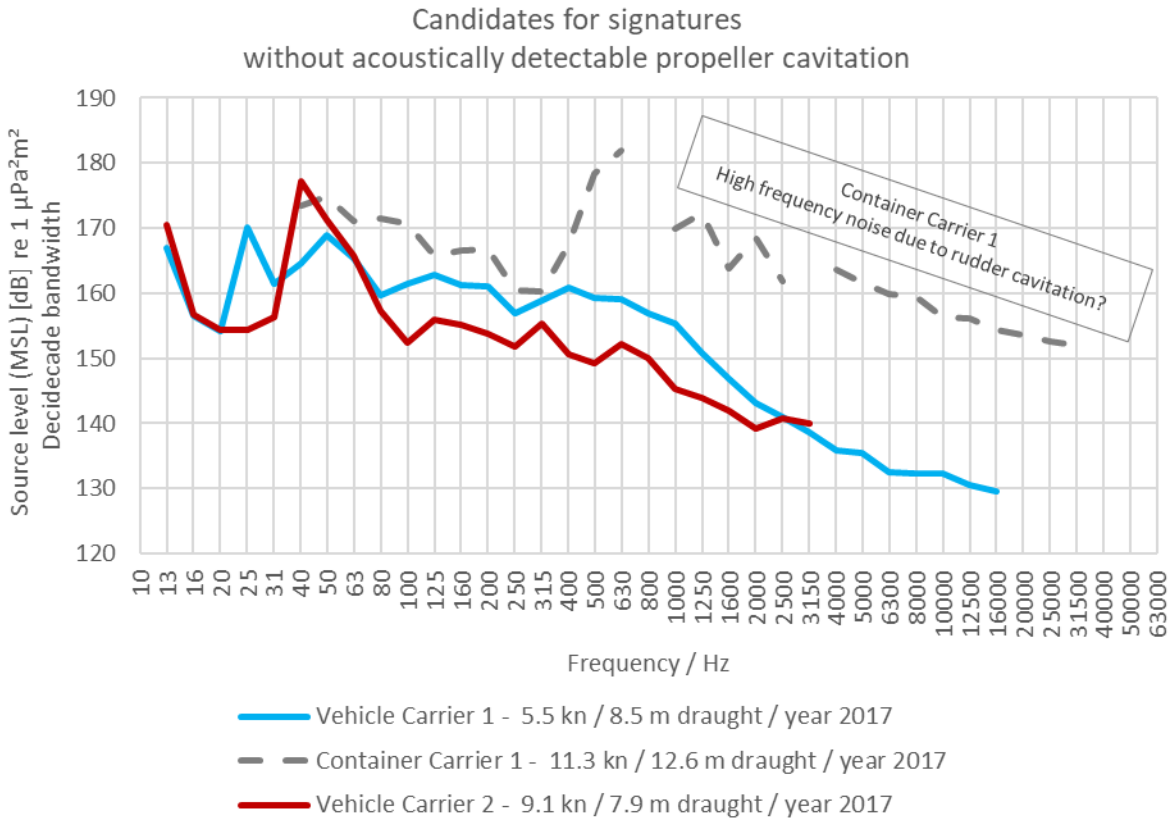

Figure 37. Decidecade source level spectra of measurements without acoustically detectable propeller cavitation. Missing monopole source level (MSL) data correspond to bands rejected due to high background noise, identified during ShipSound quality checks.

Table 6. Summary of manual analysis of underwater noise acoustic measurements to determine the presence of cavitation noise.

STW	Engine audible?	LF continuous broadband audible?	HF smooth broadband sound audible?	HF "crisp" sound audible?	HF sharp transients audible	Other comment	Dominant modulation source	Cavitation?
Bulker 1 (General Cargo)								
9.4	No	Repetitive once per rev, well visible in spectrogram around 60 Hz	Yes	Incipient crisp	No	--	Main engine, sporadic cavitation	Yes
14.4	No	Repetitive once per rev at 90 Hz, continuous around 60 Hz	Yes, only one blade per rev	Continuous crisp	No	--	Propeller cavitation, dominant LF cavitation	Yes
16.5	No	Yes, very strong	Once per rev	Yes, audible after CPA	No	--	Propeller cavitation	Yes
Tanker 1								
10.2	at CPA: no far after CPA: yes	Difficult to distinguish from engine	Smooth modulation of all blades (no distinct exception due to damage)	Very weak	No	Sometimes transient HF “crisp” noise	Main engine & propeller	Yes
13.1	No	Yes, without modulation	Audible modulation with one strongest event out of 5	NO	Yes, audible only after CPA	Squeaking (shaft bearing?)	Continuous HF broadband cavitation w/o distinct amplitude modulation	Yes
15.0	No	Yes, no modulation	No	NO	yes, pronounced and constantly	squeaking	Each blade cavitation with multiple heavy impulses per revolution. RPM cannot clearly be quantified.	Yes
Vehicle Carrier 1								
5.5	Individual cylinders audible, repetitive pressurized air blow off (indicator for overall low level of cavitation noise)	No	No	Slightly, only in CPA, modulated	No	Dominant noise floor from auxiliary machinery, gearbox or pump audible before CPA, not audible after CPA	Main engine	No
13.8	Yes, repetitive modulated HF noise	Yes	Pronounced once per blade	Slightly, only in CPA, modulated	No	--	Propeller 5 blades	Yes
18.1	No	Yes	Yes, clear modulation audible in all positions	Yes, modulated with unsteady pattern	Slightly audible in all positions		Propeller 5 blades	Yes

Vehicle Carrier 2								
9.1	Yes	Yes	Continuous	No	No	Contaminated by cetacean clicks & vocalizations	Main engine (weak)	No
15.8	No	Yes	Yes, quiet, with modulation at shaft rpm	Yes, audible with modulation at blade frequency	No	--	Propeller HF cavitation	Yes
19.8	No	No	Yes, quiet, without modulation	Yes, very pronounced audible with modulation at blade frequency	No	--	Propeller HF transients	Yes
Vehicle Carrier 3								
10.8	Slightly in aft position	No	Yes, without modulation	No	No	Mechanical rattling randomly audible	Main engine & “crisp” cavitation	Yes
16.5	No	Yes	Yes, with modulation audible in positions bow / abeam / aft	Yes, with modulation audible in all positions	No	--	Continuous LF & HF broadband cavitation, no clear amplitude modulation	Yes
19.5	No	Yes	Yes, mostly masked by crisp sounds	Yes, modulated with random structure	No	--	Fully cavitating, sporadic impulsive cavitation	Yes
Container Carrier 1								
11.3	No (masked by propeller singing)	No	No	No	No	Propeller singing with modulation, masking other sounds during listening	Propeller singing, main engine	Likely only rudder cavitation
16.9	No	Yes	Yes, very quiet	Yes, with modulation audible in all positions	No	--	Propeller HF cavitation	Yes
22.3	No	Yes	Yes, without modulation	Yes, modulated	Yes, randomly at varying amplitude	--	Propeller cavitation	Yes
Container Carrier 2								
11.9	Yes, only at low frequency, high repetition	No	Strong modulation with clear disappearance in between blades, each blade very similar amplitude	Incipient crisp, randomly occurring alongside with modulated smooth broadband	No	Very similar impression in positions bow, abeam, aft	Main engine & HF propeller cavitation	Yes

17.7		Incipient upsweep below 100 Hz	Continuous broadband with weak modulation	Modulated crisp heard only from bow position	Each blade features very similar transient, stable over full passage, very small tolerances in repetition rate, audible in positions abeam and aft	--	HF propeller cavitation	Yes
20.0		Dominant upsweep below 100 Hz	Modulation well audible form bow position, less pronounced abeam and aft	Modulated crisp audible from bow	Weak transients audible from aft position	--	LF & HF propeller cavitation	Yes
Container Carrier 3								
10.6	Yes	No	Strong modulation with clear disappearance in between blades, audible in all positions	No	No	--	Main engine & HF propeller cavitation	Yes
16.7	No	No	Yes, without modulation	Yes, with unclear modulation pattern	Yes, weak and random	--	HF propeller cavitation	Yes
20.0	No	Yes	Yes, without modulation	No	Yes, repetitive with blade frequency	--	HF propeller cavitation	Yes
Container Carrier 4								
10.0	Yes, repetitive below few kHz	No	Bow position: Strong modulation with clear disappearance in between blades, each blade very similar amplitude, modulation less pronounced towards aft position	no	No	--	Main engine, HF propeller cavitation	Yes
18.0	No	Yes, similar in all positions	yes, free of modulation in all positions	No	No	Waveform shows nearly constant rms amplitude over full passage	None	Yes
21.6	No	Yes	Yes, very little modulation in all positions	Yes, only abeam	No	--	Propeller cavitation	Yes

Container Carrier 5								
9.5	Yes	No	Strong modulation with clear disappearance in between blades, audible in all positions	No	No	--	Main engine, propeller cavitation	Yes
17.2	No	Yes	Yes, free of modulation in all positions	Slightly in aft position	No	--	HF propeller cavitation	Yes
20.7	No	Yes, very strong	Continuous HF broadband, mechanical rattling	No	No	Mechanical rattling, low frequency flow noise & vocalizations	LF & HF propeller cavitation	Yes

3. Discussion

3.1. Descriptor Evaluation

Of the five CIS descriptors analyzed in this work, the following three performed successfully (i.e., as hypothesized):

- **Descriptor 1** (Increase in low-frequency cavitation hump): This descriptor yielded reasonable CIS estimates because it established a relationship between the URN data and an empirical model for the noise mechanisms driving the cavitation hump at low frequencies. Descriptor 1 gave reasonable estimates of the onset of low-frequency cavitation noise, using the entire data ensemble (per vessel category) and applied individually to vessels spanning a velocity range sufficient to constraint the model.
- **Descriptor 2** (Tonal count): This descriptor performed as hypothesized for all vessel categories except Tankers. It performed particularly well for Container Ship and Vehicle Carrier categories, showing a clear transition from high to low tonal count at approximately 12 kn STW. For Bulkers, there appeared to be a trend with speed, consistent with the experimental hypothesis, but there was no clear transition point.
- **Descriptor 3** (Spectral slope): This descriptor performed as hypothesized for Container Ship and Vehicle Carrier categories; however, it did not exhibit a clear inflection point indicating onset of CIS. In many examples with sufficient speed range span, the spectral slope followed the expected behaviour: steep slopes in the absence of cavitation, and flatter slopes during high cavitation. However, visual inspection of the results for each vessel suggests that the spectral slope value at low or high cavitation is unique for each vessel, which makes it difficult to establish a CIS criterion based on specific slope values. For example, a slope of −20 dB/$\log_{10}$ Hz could indicate low cavitation for one vessel but high cavitation for another vessel.

These three descriptors required multiple measurements of a single vessel operating at a wide range of speeds. The two remaining descriptors did not perform as hypothesized and were therefore discarded from further consideration:

- **Descriptor 4** (Factor X of URN increase relative to speed): Although the principle behind this descriptor is sound, the definition of the descriptor by a local point-to-point slope results in high variability. In addition, the descriptor relies on an accurate reference measurement at low speed, which is not always available.
- **Descriptor 5** (Confidence of dual-band RPM estimator): This descriptor did not yield a clear data clustering to distinguish between data with and without cavitation. In principle, analysis of the DEMON spectra should give solid clues on the presence or absence of cavitation. However, the confidence factor as defined by the RPM algorithm is focused on judging the quality of the RPM estimate, as opposed to the quality of the DEMON and low-frequency spectra. Customizing the algorithm to target detecting cavitation is a possible future avenue for investigation.

Note that the two most successful descriptors (1 and 2) were sensitive only to the low-frequency region of the cavitation spectrum (i.e., below 100 Hz). As discussed in Section 2.3 and confirmed by manual analysis, the initial onset of cavitation noise (i.e., Condition 2 in Figure 4) occurs at high frequencies and generally precedes the onset of cavitation noise at low frequencies (i.e., Conditions 3 and 4 in Figure 4). While the 0.1–20 kHz spectral slope (Descriptor 3) did cover the high-frequency part of the spectrum, this descriptor was more difficult to interpret because it exhibited considerable variability between vessels and

had no clear inflection point. Incipient cavitation was detected in manual analysis, which showed that modulated high-frequency broadband sound of incipient cavitation can be similar to sounds of the two-stroke main engine at slow speed. Thus, it is likely that CIS estimates obtained using these descriptors correspond to the onset of fully developed cavitation with contribution below 1 kHz and strong increase of levels at higher frequencies rather than incipient cavitation with weaker contribution only in the kHz frequency range. Notwithstanding these limitations, Descriptors 1–3 were incorporated into a rudimentary CIS estimation criterion based on the results of the implementation study.

3.2. CIS Criterion

Of the three successful CIS descriptors, only Descriptor 1 lends itself to unambiguous estimation of an actual CIS estimate by defining CIS as the speed at which the underlying cavitation model exceeds the machinery model. Whether this is an appropriate threshold to indicate the presence of cavitation in a URN measurement remains uncertain. Analysis of raw audio data by a human analyst (Section 2.7) suggests this method likely underestimates the true CIS due to its reliance on the low-frequency spectrum of the measurements related more closely to fully developed cavitation. The non-linear least squares algorithm performed best when applied to individual vessels, yielding the CIS estimates presented in Table 4 per vessel category.

Descriptors 2 and 3 were useful for providing supporting evidence of underlying processes shaping the spectrum as the vessel speed increased. For most vessel categories, their outputs showed the expected trend when going from low to high speeds, but there was no clear breakpoint that could be taken as a CIS estimator. To distill these descriptors into a single true or false criterion, we applied a statistical hypothesis test (Student's t-test) to the outputs of Descriptors 2 and 3, using the mean CIS from Descriptor 1 as a breakpoint, to provide additional evidence of consistency between the three estimators. Thus, we applied a hypothesis test as follows:

- For each vessel category, the mean Descriptor 1 CIS in Table 4 was used to split the tone count (Descriptor 2) and spectral slope (Descriptor 3) data in each vessel category into two groups: below and above mean CIS.
- The t-test was applied to the two groups to determine if the mean descriptor value below and above CIS can be considered as belonging to different populations (interpreted as predominantly cavitating and non-cavitating vessels).

Figure 38 shows box plots of the tonal count, split below and above the mean CIS from Descriptor 1. The p-value results from the t-test are shown in each panel. In all cases, p-values were below 0.001, which is considered strong evidence in support of the hypothesis that the tone counts are different above and below the estimated CIS. The magnitude of the difference was largest for Container Vessels and Vehicle Carriers (averaging 11.0 and 12.6 more tonals, respectively, below the mean CIS from Descriptor 1, than above it). The magnitude of the difference was smaller, but nonetheless statistically significant, for Bulkers (averaging 3.3 more tonals below the mean CIS from Descriptor 1, than above it) owing principally to the large number of measurements in this category. The difference for Tankers, while statistically significant, was negative and thus inconsistent with the experimental hypothesis. Thus, the hypothesis tests for Descriptor 2 provided supporting evidence for CIS estimates in three of four vessel categories. While the populations were statistically different, there was still significant overlap between the two populations (below CIS and above CIS from Descriptor 1).

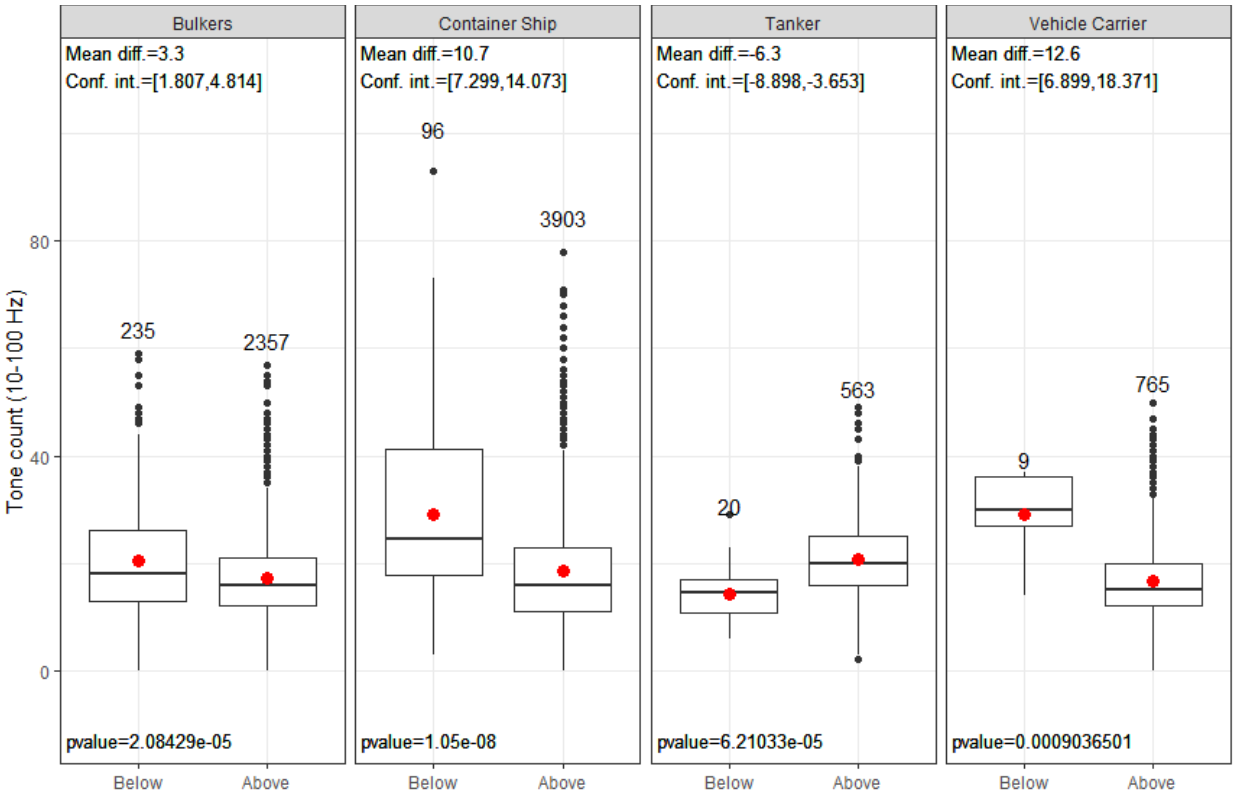

Figure 38. Distribution of the tonal count for measurements below and above the mean Cavitation Inception Speed (CIS) in Table 4. The red dot indicates the mean value of each box. A t-test was applied to each (below versus above) subset to determine if their means are statistically different. The difference in the mean below and above CIS is shown in the legend, followed by the confidence interval and the p-value for the t-test.

Similar to Descriptor 2, we tested the consistency between the mean CIS from Descriptor 1 and the 0.1–20 kHz spectral slope from Descriptor 3, using a t-test. Figure 39 shows box plots of the spectral slope, split below and above the mean CIS. Only the p-values for the Container Ship and Vehicle Carrier categories support the hypothesis of statistically different means below and above the estimated CIS. The p-value for Tankers indicated that the difference in Descriptor 2 was statistically significant, but in the opposite direction to the hypothesized trend. The reason for this result is currently unknown but may be related to regulations that require Tankers to be accompanied by escort tugs when travelling at speeds less than 10 knots (i.e., because tug noise would interfere with attempts to measure CIS). Thus, the hypothesis tests for Descriptor 3 provided supporting evidence for CIS estimates in two of four vessel categories. Like the results from Descriptor 2, while there was a statistically significant difference there was also significant overlap.

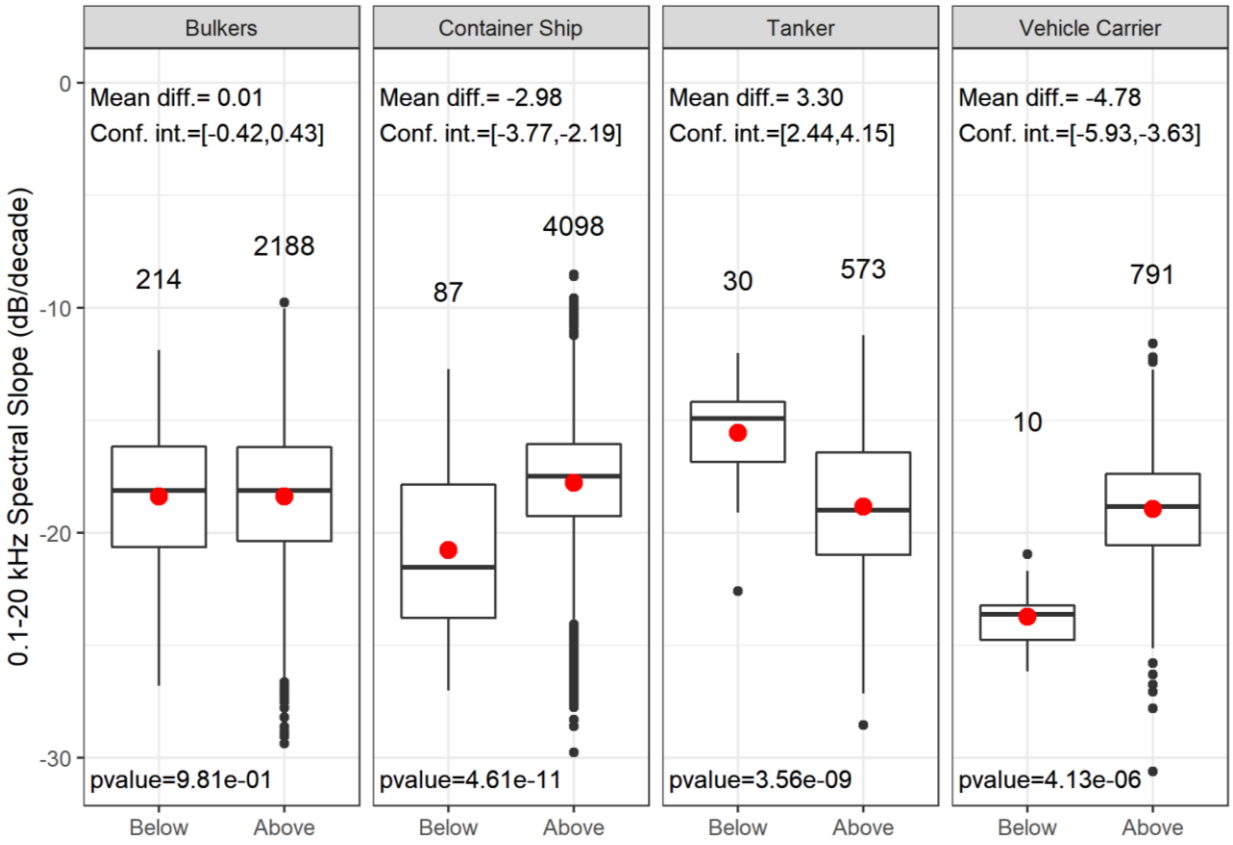

Figure 39. Distribution of the 0.1–20 kHz spectral slope for measurements below and above the mean Cavitation Inception Speed (CIS) in Table 4. The red dot indicates the mean value of each box. A t-test was applied to each (below versus above) data subset pair, to determine if their means are statistically different. The difference in the mean below and above CIS is shown in the legend, followed by the confidence interval and the p-value for the t-test.

3.3. Limitations and Future Work

The main limitation in this analysis is the general lack of measurements at speeds below 10 kn. This is due mostly to the speed specifications by the shipping operators, as well as inherent ship operational specifications for each vessel type. Until a more direct method to detect cavitation is implemented (i.e., an automated cavitation noise detector with a human analysist for ground truthing), the results in this report offer the best CIS estimates assuming the underlying noise model proposed for Descriptor 1.

Prior experience suggests that an automated cavitation detection algorithm is feasible because, in addition to the descriptors developed here, there are several other spectral features present when cavitation is developed, as has been pointed out by other studies (McIntyre 2021). For example, cavitation tends to cause wide ‘skirts’ around usually narrow machinery harmonics. Other authors have recently suggested the use of spectral kurtosis (a signal processing technique for the detection of non-stationary noise bursts embedded in continuous noise, see Glossary) as a preliminary step for cavitation enhancement (Lee and Seo 2013). The use of Detection of Envelope MOdulation on Noise (DEMON) is still a promising approach, and it may warrant investigating fine tuning the algorithm for cavitation detection (rather than for shaft rate estimation).

4. Conclusions

The main findings of the CIS implementation study are summarized as follows:

- Of the five noise descriptors evaluated in this study, three yielded results that were consistent with the experimental hypotheses:
  - **Descriptor 1** (Increase in low-frequency cavitation hump (20–80 Hz)): This descriptor yielded reasonable CIS estimates for all four vessel categories because it established a relationship between the URN data and an empirical model for the noise mechanisms driving the cavitation hump below 100 Hz.
  - **Descriptor 2** (Number of tonals below 100 Hz): This descriptor exhibited a clear inflection point at approximately 12 kn for Container Ships and Vehicle Carriers. A weak trend, but no inflection point, was observed for Bulkers, and results for Tankers were inconclusive.
  - **Descriptor 3** (Spectral slope (0.1–20 kHz)): This descriptor exhibited a clear trend for Container Ships and Vehicle Carriers but had no inflection point. Results for Bulkers were inconclusive. The trend of this descriptor was contrary to the hypothesized trend for Tankers, for reasons which are unknown at present.
- The two remaining noise descriptors yielded results that were inconclusive or inconsistent with the experimental hypotheses and were dropped from further consideration:
  - **Descriptor 4** (Factor X of URN increase relative to speed): This descriptor proved too variable, even after binning, to yield useful interpretations.
  - **Descriptor 5** (Confidence of dual-band RPM detector): Results for this descriptor did not exhibit a conclusive trend. However, it is likely that the confidence factor could be improved on by focusing on quality of the cavitation spectrum rather than on the RPM estimate.
- A CIS criterion was developed by combining Descriptors 1–3 using statistical hypothesis testing (see Table 7). This method yielded good quality CIS estimates for Container Ships and Vehicle Carriers but only moderate and poor quality CIS estimates for Bulkers and Tankers, respectively.
- The successful descriptors were most sensitive to low-frequency (<100 Hz) features of the URN spectrum. Thus, it is likely the that the CIS estimates they yielded (Table 7) correspond to onset of fully-developed cavitation rather than incipient cavitation
- The lack of URN data at low speeds limited the ability of the descriptors to yield a more precise CIS estimate. This issue was particularly acute for Bulkers and Tankers, which were mostly measured over a relatively narrow speed range.
- The use of Detection of Envelope MOdulation on Noise (DEMON) is still a promising approach and may warrant an investigation into fine tuning the algorithm for cavitation detection in future.
- Manual analysis of 30 vessel measurements found only 2 measurements without cavitation, both of which were obtained at very low speeds (less than 10 knots STW). This suggests that a large majority of the measurements in the data set were obtained above the cavitation inception speed. Furthermore, this suggests that statistical analysis of the acoustic descriptors likely overestimated the cavitation inception speed for vessels in the data set, due to a paucity of data for cavitation-free conditions and the reliance on low-frequency cavitation for the estimation of CIS by two of the three descriptors included in the CIS criterion. Low-frequency cavitation is more reflective of fully developed cavitation than cavitation inception (Condition 5 versus Condition 2 from Section 2.3).

Table 7. Results obtained from implementation of a Cavitation Inception Speed (CIS) criterion, based on analysis of noise descriptors 1–3. The score in the last column is a ranking of the quality of the mean CIS estimate based on the number of descriptors supporting the estimated value.

Category	Mean CIS estimate (Descriptor 1)	Supported by 10–100 Hz tone count (Descriptor 2)	Supported by 0.1–20 kHz spectral slope (Descriptor 3)	Score
Bulkers	11.2 ± 0.7	Yes	No	2 (Moderate)
Container Ships	12.0 ± 2.3	Yes	Yes	3 (Good)
Tankers	10.1 ± 1.1	No	No	1 (Poor)
Vehicle Carriers	11.0 ± 3.0	Yes	Yes	3 (Good)

Glossary

Unless otherwise stated in an entry, these definitions are consistent with ISO 18405 (2017).

1/3-octave

One third of an octave. *Note*: A 1/3-octave is approximately equal to one decidecade (1/3 oct ≈ 1.003 ddec).

1/3-octave-band

Frequency band whose bandwidth is one 1/3-octave. *Note*: The bandwidth of a 1/3-octave-band increases with increasing centre frequency.

absorption

The conversion of sound energy to heat energy. Specifically, the reduction of sound pressure amplitude due to particle motion energy converting to heat in the propagation medium.

acoustic noise

Sound that interferes with an acoustic process.

ambient sound

Sound that would be present in the absence of a specified activity (ISO 18405:2017). Usually a composite of sound from many sources near and far, e.g., shipping vessels, seismic activity, precipitation, sea ice movement, wave action, and biological activity.

attenuation

The gradual loss of acoustic energy from absorption and scattering as sound propagates through a medium. Attenuation depends on frequency—higher frequency sounds are attenuated faster than lower frequency sounds.

background noise

Combination of ambient sound, acoustic self-noise, and, where applicable, sonar reverberation (ISO 18405:2017) that is detected, measured, or recorded with a signal.

bandwidth

A range within a continuous band of frequencies. Unit: hertz (Hz).

box-and-whisker plot

A statistical data plot that illustrates the centre, spread, and overall range of data as a visual 5-number summary. The box is the interquartile range (IQR), which shows the middle 50 % of the data—from the lower quartile (25th percentile) to the upper quartile (75th percentiles). The line inside the box is the median (50th percentile). The whiskers show the lower and upper extremes excluding outliers, which are data points that fall more than 1.5 × IQR beyond the upper or lower quartiles.

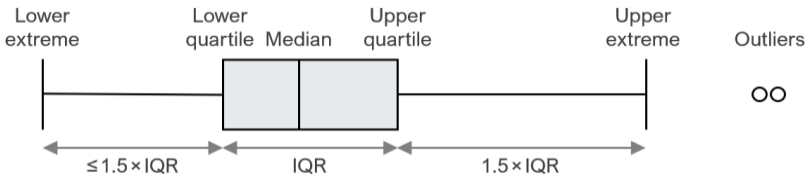

boxcar averaging

A signal smoothing technique that returns the averages of consecutive segments of a specified width.

broadband level

The total level measured over a specified frequency range. If the frequency range is unspecified, the term refers to the entire measured frequency range.

cavitation

A rapid formation and collapse of vapor cavities (i.e., bubbles or voids) in water, most often caused by a rapid change in pressure. Fast-spinning vessel propellers typically cause cavitation, which creates a lot of noise.

continuous sound

A sound whose sound pressure level remains above the background noise during the observation period and may gradually vary in intensity with time, e.g., sound from a marine vessel.

decade

Logarithmic frequency interval whose upper bound is ten times larger than its lower bound (ISO 80000-3:2006). For example, one decade up from 1000 Hz is 10,000 Hz, and one decade down is 100 Hz.

decibel (dB)

Unit of level used to express the ratio of one value of a power quantity to another on a logarithmic scale. Especially suited to quantify variables with a large dynamic range.

decidecade

One tenth of a decade. Approximately equal to one third of an octave (1 ddec ≈ 0.3322 oct), and for this reason sometimes referred to as a 1/3-octave.

decidecade band

Frequency band whose bandwidth is one decidecade. *Note*: The bandwidth of a decidecade band increases with increasing centre frequency.

frequency

The rate of oscillation of a periodic function measured in cycles per unit time. The reciprocal of the period. Unit: hertz (Hz). Symbol: f. 1 Hz is equal to 1 cycle per second.

harmonic

A sinusoidal sound component that has a frequency that is an integer multiple of the frequency of a sound to which it is related. For a sound with a fundamental frequency of f, the harmonics have frequencies of $2f$, $3f$, $4f$, etc.

hertz (Hz)

Unit of frequency defined as one cycle per second. Often expressed in multiples such as kilohertz (1 kHz = 1000 Hz).

hydrophone

An underwater sound pressure transducer. A passive electronic device for recording or listening to underwater sound.

hydrostatic pressure

The pressure at any given depth in a static liquid that is the result of the weight of the liquid acting on a unit area at that depth, plus any pressure acting on the surface of the liquid. Unit: pascal (Pa).

intermittent sound

A sound whose level abruptly drops below the background noise level multiple times during an observation period.

impulsive sound

Qualitative term meaning sounds that are typically transient, brief (less than 1 s), broadband, with rapid rise time and rapid decay. They can occur in repetition or as a single event. Sources of impulsive sound include, among others, explosives, seismic airguns, and impact pile drivers.

knot (kn)

Unit of vessel speed equal to 1 nautical mile per hour.

level

A measure of a quantity expressed as the logarithm of the ratio of the quantity to a specified reference value of that quantity. For example, a value of sound pressure level with reference to 1 μPa^2 can be written in the form *x* dB re 1 μPa^2.

manual analysis

Human examination of acoustic data via visual review of spectrograms and/or aural inspection of data.

masking

Obscuring of sounds of interest by other sounds at similar frequencies.

median

The 50th percentile of a statistical distribution.

monopole source level (MSL)

A source level that has been calculated using an acoustic model that accounts for the effect of the sea-surface and seabed on sound propagation, assuming a point source (monopole). Often used to quantify source levels of vessels or industrial operations from measurements. See also radiated noise level.

multiple linear regression

A statistical method that seeks to explain the response of a dependent variable using multiple explanatory variables.

non-impulsive sound

Sound that is not an impulsive sound. Not necessarily a continuous sound.

octave

The interval between a sound and another sound with double or half the frequency. For example, one octave above 200 Hz is 400 Hz, and one octave below 200 Hz is 100 Hz.

percentile level

The sound level not exceeded *N* % of the time during a specified time interval. The *N*th percentile level is equal to the (100−*N*) % exceedance level. See also N percent exceedance level.

point source

A source that radiates sound as if from a single point.

power spectral density

Generic term, formally defined as power in a unit frequency band. Unit: watt per hertz (W/Hz). The term is sometimes loosely used to refer to the spectral density of other parameters such as squared sound pressure. Ratio of energy spectral density, E_f, to time duration, Δt, in a specified temporal observation window. In equation form, the power spectral density P_f is given by $P_f = E_f/\Delta t$. Power spectral density can be expressed in terms of various field variables (e.g., sound pressure, sound particle displacement).

power spectral density level

The level ($L_{P,f}$) of the power spectral density (P_f) in a stated frequency band and time window. Defined as: $L_{P,f} = 10log_{10}(P_f/P_{f,0})$. Unit: decibel (dB).

As with power spectral density, power spectral density level can be expressed in terms of various field variables (e.g., sound pressure, sound particle displacement). The reference value ($P_{f,0}$) for power spectral density level depends on the nature of the field variable.

power spectral density source level

A property of a sound source equal to the power spectral density level of the sound pressure measured in the far field plus the propagation loss from the acoustic centre of the source to the receiver position. Unit: decibel (dB). Reference value: 1 $\mu Pa^{2\ m2}$/Hz.

propagation loss (PL)

Difference between a source level (SL) and the level at a specified location, $\mathrm{PL}(x) = \mathrm{SL} - L(x)$. Unit: decibel (dB). See also transmission loss.

propeller singing

Tonal sound radiated by the propeller at high level. Propeller singing can occur if a natural frequency of a propeller blade is excited by vortex shedding at the trailing edge of propeller blades. This can generate high amplitudes as excitation of the vortex and response of the blade are amplifying each other in feedback.

radiated noise level (RNL)

A source level that has been calculated assuming sound pressure decays geometrically with distance from the source, with no influence of the sea-surface or seabed. Often used to quantify source levels of vessels or industrial operations from measurements. See also monopole source level.

received level

The level of a given field variable measured (or that would be measured) at a given location.

reference value

Standard value of a quantity used for calculating underwater sound level. The reference value depends on the quantity for which the level is being calculated:

Quantity	Reference value
Sound pressure	p_0^2 = 1 μPa^2 or p_0 = 1 μPa
Sound exposure	E_0 = 1 μPa^2 s
Sound particle displacement	δ_0^2 = 1 pm^2
Sound particle velocity	u_0^2 = 1 nm^2/s^2
Sound particle acceleration	a_0^2 = 1 μm^2/s^4

sound

A time-varying disturbance in the pressure, stress, or material displacement of a medium propagated by local compression and expansion of the medium. In common meaning, a form of energy that propagates through media (e.g., water, air, ground) as pressure waves.

sound exposure

Time integral of squared sound pressure over a stated time interval in a stated frequency band. The time interval can be a specified time duration (e.g., 24 h) or from start to end of a specified event (e.g., a pile strike, an airgun pulse, a construction operation). Unit: pascal squared second (Pa^2 s). Symbol: E.

sound exposure level (SEL)

The level (L_E) of the sound exposure (E) in a stated frequency band and time window: $L_E = 10\log_{10}(E/E_0)$ (ISO 18405:2017). Unit: decibel (dB). Reference value (E_0) for sound in water: 1 μPa^2 s.

sound exposure spectral density

Distribution as a function of frequency of the time-integrated squared sound pressure per unit bandwidth of a sound having a continuous spectrum (ISO 18405:2017). Unit: pascal squared second per hertz (Pa^2 s/Hz).

sound field

Region containing sound waves.

sound pressure

The contribution to total pressure caused by the action of sound (ISO 18405:2017). Unit: pascal (Pa). Symbol: p.

soundscape

The characterization of the ambient sound in terms of its spatial, temporal, and frequency attributes, and the types of sources contributing to the sound field (ISO 18405:2017).

source level (SL)

A property of a sound source equal to the sound pressure level measured in the far field plus the propagation loss from the acoustic centre of the source to the receiver position. Unit: decibel (dB). Reference value: 1 $\mu Pa^{2\,m2}$.

spectral kurtosis

A signal processing technique for the detection of non-stationary noise bursts embedded in continuous noise (Lee and Seo 2013). Since propeller cavitation manifest itself as noise bursts with a repetition rate determined by the propeller rate, spectral kurtosis has been proposed as a method to determine the optimal frequency band where cavitation is the loudest.

spectrogram

A visual representation of acoustic amplitude over time and frequency. A spectrogram's resolution in the time and frequency domains should generally be stated as it determines the information content of the representation.

spectrum

Distribution of acoustic signal content over frequency, where the signal's content is represented by its power, energy, mean-square sound pressure, or sound exposure.

transmission loss (TL)

The difference between a specified level at one location and that at a different location: $\mathrm{TL}(x_1,x_2) = L(x_1) - L(x_2)$ (ISO 18405:2017). Unit: decibel (dB). See also propagation loss.

wavelength

Distance over which a wave completes one cycle of oscillation. Unit: metre (m). Symbol: λ.

Literature Cited

[ISO] International Organization for Standardization. 2006. *ISO 80000-3:2006 Quantities and units – Part 3: Space and time*. https://www.iso.org/standard/31888.html.

[ISO] International Organization for Standardization. 2017. *ISO 18405:2017. Underwater acoustics – Terminology*. Geneva. https://www.iso.org/standard/62406.html.

[ISO] International Organization for Standardization. 2019. *ISO 17208-2:2019. Underwater acoustics — Quantities and procedures for description and measurement of underwater sound from ships — Part 2: Determination of source levels from deep water measurements*. https://www.iso.org/standard/62409.html.

Baiter, H.-J. 1992. *Advance views of cavitation noise*. *International Symposium on Propulsors and Cavitation* 1992, Hamburg, Germany.

Bedford Institute of Oceanography. 2015. *WebTide Tidal Prediction Model (v0.7.1)* (web page). Government of Canada. http://www.bio-iob.gc.ca/science/research-recherche/ocean/webtide/index-en.php.

Carlton, J. 2012. *Marine Propellers and Propulsion* 3rd edition. Elsevier Butterworth Heinemann https://www.elsevier.com/books/marine-propellers-and-propulsion/carlton/978-0-08-097123-0.

Collins, M.D. 1993. A split-step Padé solution for the parabolic equation method. *Journal of the Acoustical Society of America* 93(4): 1736-1742. https://doi.org/10.1121/1.406739.

Daniel, J., M. Schuster, J.E. Quijano, J.N. Dolman, and A.O. MacGillivray. 2022. *ECHO Cavitation Inception Speed Study—Phase 1: Task 2 Technical Report*. Document 02783, Version 2.0. Technical report by JASCO Applied Sciences and DW-ShipConsult GmbH for Vancouver Fraser Port Authority.

François, R.E. and G.R. Garrison. 1982a. Sound absorption based on ocean measurements: Part II: Boric acid contribution and equation for total absorption. *Journal of the Acoustical Society of America* 72(6): 1879-1890. https://doi.org/10.1121/1.388673.

François, R.E. and G.R. Garrison. 1982b. Sound absorption based on ocean measurements: Part I: Pure water and magnesium sulfate contributions. *Journal of the Acoustical Society of America* 72(3): 896-907. https://doi.org/10.1121/1.388170.

Hosien, M.A. and S.M. Selim. 2017. Acoustic Detection of Cavitation Inception. *Journal of Applied Fluid Mechanics* 10(1): 31-40. https://doi.org/10.18869/acadpub.jafm.73.238.25638.

JASCO Applied Sciences and SMRU Consulting. 2020. *ECHO Program 2019 Voluntary Vessel Slowdown Hydroacoustic Studies: Final Report*. Document 01994, Version 1.0. Technical report by JASCO Applied Sciences and SMRU Consulting for Vancouver Fraser Port Authority (VFPA). https://www.portvancouver.com/wp-content/uploads/2020/08/ECHO-Program-2019-voluntary-vessel-slowdown-in-Haro-Strait-and-Boundary-Pass-final-report.pdf.

Lee, J.-H. and J.-S. Seo. 2013. Application of spectral kurtosis to the detection of tip vortex cavitation noise in marine propeller. *Mechanical Systems and Signal Processing* 40(1): 222-236. https://doi.org/10.1016/j.ymssp.2013.04.002.

MacGillivray, A.O., J. Ainsworth, H. Frouin-Mouy, J.N. Dolman, and M.A. Bahtiarian. 2020a. *ECHO Vessel Noise Correlations Study: Final Report*. Document 02025, Version 2.0. Technical report by JASCO Applied Sciences, ERM, and Acentech for Vancouver Fraser Port Authority ECHO Program.

MacGillivray, A.O., J. Zhao, M.A. Bahtiarian, J.N. Dolman, J.E. Quijano, H. Frouin-Mouy, and L. Ainsworth. 2020b. *ECHO Vessel Noise Correlations Phase 2 Study: Final Report*. Document 02283, Version 1.0. Technical report by JASCO Applied Sciences, ERM, and Acentech for Vancouver Fraser Port Authority ECHO Program.

MacGillivray, A.O. and C.A.F. de Jong. 2021. A Reference Spectrum Model for Estimating Source Levels of Marine Shipping Based on Automated Identification System Data. *Journal of Marine Science and Engineering* 9(4): 369. https://doi.org/10.3390/jmse9040369.

MacGillivray, A.O., L.M. Ainsworth, J. Zhao, J.N. Dolman, D.E. Hannay, H. Frouin-Mouy, K.B. Trounce, and D.A. White. 2022. A functional regression analysis of vessel source level measurements from the Enhancing Cetacean Habitat and Observation (ECHO) database. *Journal of the Acoustical Society of America* 152(3): 1547-1563. https://doi.org/10.1121/10.0013747.

McIntyre, D. 2021. *Predicting Cavitation-Induced Noise from Marine Propellers*. MSc Thesis. University of Victoria. https://dspace.library.uvic.ca/bitstream/handle/1828/12552/McIntyre_Duncan_MASc_2020.pdf?sequence=3&isAllowed=y.

R Core Team. R: A language and environment for statistical computing. R Foundation for Statistical Computing, Vienna, Austria. http://www.R-project.org/.

Seeber, B.U. 2008. Masking and Critical Bands. *In* Havelock, D., S. Kuwano, and M. Vorländer (eds.). *Handbook of Signal Processing in Acoustics*. Springer New York, New York. pp. 229-240. https://doi.org/10.1007/978-0-387-30441-0_16.

Zheng, C., D. Liu, and H. Huang. 2019. The Numerical Prediction and Analysis of Propeller Cavitation Benchmark Tests of YUPENG Ship Model. *Journal of Marine Science and Engineering* 7(11): 387. https://doi.org/10.3390/jmse7110387.

Appendix A. PortListen®

The acoustic recordings from the ULS were analyzed using PortListen, JASCO's custom vessel noise measurement system.

The acoustic data were analyzed in 1/3-octave frequency bands from 10 Hz to 64 kHz. Each sound recording was processed using 1-s sliding Fast Fourier Transforms (FFTs) applied with a power-normalized Hanning window, with 50 % overlap, to obtain power spectral density (PSD) levels versus time. The 1/3-octave-band received levels (RL) were computed by band-pass filtering the 1-s PSD data into 1/3-octave frequency bins. The vessel tracks were obtained from Automatic Identification System (AIS) data. Since the AIS transmitter/receiver was not necessarily coincident with a vessel's acoustic source, the acoustic closest point of approach (CPA) was determined by tracking the range and speed of the source using an automated tracking algorithm based on the cepstrogram method. The background noise levels (NL) were computed by averaging noise levels over two 1-min intervals—1 min just before a vessel entered the entrance funnel and 1 min after it left the exit zone. Measured RLs were compared with the NLs in 1/3-octave-band frequencies and were adjusted as needed based on the method prescribed in ANSI 12.64-2009.

The source levels were computed along the track with a ±30° azimuth angle centred from the acoustic CPA. The computation of source levels requires analyzing the measurements made at a distance, typically of a few hundred metres, and scaling them to account for the propagation loss that occurs as the sound propagates from source to the receiver location. The PortListen system calculates both Radiated Noise Level (RNL) and Monopole Source Level (MSL). RNL is calculated by applying spherical spreading loss 20log(R), where R is the slant measurement range in metres. The RNL method neglects sound reflecting off the sea surface and the seabed. Those reflections introduce important propagation effects, especially for frequencies below ~250 Hz. The MSL calculation accounts for these reflection effects and is computed using propagation loss from JASCO's Marine Operation Noise Model (MONM). MONM computes sound propagation loss in range-varying acoustic environments through a wide-angle parabolic equation (PE) solution to the acoustic wave equation (Collins 1993). MONM accounts for the environmental parameters including water depth, seabed geoacoustic parameters, and water sound speed profile (SSP). For both RNL and MSL, the attenuation of acoustic energy by molecular absorption in seawater was also considered and computed using the formulae of François and Garrison (1982a, 1982b).

The RNLs and MSLs (broadband and 1/3-octave-band) were computed in decibels as a linear average from the RNLs and MSLs from all 1-s sample locations along the vessel track within the ±30° data window as defined in ANSI 12.64-2009.

PortListen

Underwater sound measurement system for harbours and waterways

Underwater noise management solution for the marine transport industry and environmental regulators

JASCO APPLIED SCIENCES

With vessel traffic on the rise at ports and terminals around the globe, the need to understand and mitigate the effects of underwater vessel noise on marine species is becoming ever more critical. Leveraging our experience as a premier provider of marine noise monitoring and assessment services, JASCO has developed PortListen, an integrated and modular solution for monitoring vessel sound emissions. With PortListen, we help stakeholders understand and manage the impact of underwater noise on marine life.

An Acoustic Weigh-in: Automatic Source Level Measurements

Analogous to a commercial vehicle weigh station, the PortListen underwater listening station measures the acoustic signature of a vessel as it passes through a defined measurement zone, typically about 2 km long by 300 m wide. The acoustic data are automatically processed and results are made available online in real-time, including radiated noise levels conforming to the ANSI 12.64 2009 (R2014) measurement standards, monopole source levels for direct use by acoustic propagation models for predicting exposures and possible effects of noise on marine fauna, frequency spectrum, and spectrograms for the entire vessel passage and for the measurement time window. Includes a full-featured Quality Control interface.